Palestine Polytechnic University

College of Engineering

Aerodynamic CFD Analysis with Underbody tunnel

By:

Safaa Hmeedat

Supervisor:

Eng. Majdi Zalloum

Submitted to the College of Engineering

In partial fulfillment of the requirements for the

Bachelor degree in Automotive Engineering

Palestine Polytechnic University

April 2018

Palestine Polytechnic University

Hebron – Palestine

Mechanical Engineering

Aerodynamic CFD Analysis with Underbody tunnel

By the guidance of our supervisor, and by the acceptance of all members in the testing committee, this project is delivered to Mechanical Engineering Department in the college of engineering and technology, to be as fulfillment of the requirement of the department for the Bachelor's degree of Mechanical Eng. / Automotive Engineering.

Supervisor signature

…………………….

Testing committee signature

……………………… ……………………….

The head of department signature

....

Acknowledgment

I would like to express my gratitude for everyone who helps me during this project, starting with my supervisor Eng. Majdi Zalloum , Dr Hussain Amro who didn't keep any effort in encouraging me to do this job. Thanks for continues support and kind communication which great effect on my performance. Thanks with great appreciation to my families, and the "Mechanical Society".

Abstract

Vehicle safety and stability is one of the basics of the vehicle industry. That is taken seriously. In order to maintain the passengers safety and their lives. Vehicle stability is related to vehicle aerodynamics. In general when the vehicle aerodynamics is improved, the stability will be improved. In this project an underbody tunnel will be added to the vehicle. In order to increase the vehicle stability, to reduce the possibility of untipped rollover accident, especially at high speeds. A 3D car model was modeled using Solid Works software. The analysis of this problem will be done by using ANSYS software. To determine the aerodynamic characteristic like pressure, drag force, lift force, drag coefficient and lift coefficient. The objective of these project is increasing the stability of the vehicle by increasing the negative lift force after adding the underbody tunnel. The effect of underbody tunnel on the vehicle has been analyzed by using ANSYS CFX software. And due to these modification the stability will be increased. But these increased in stability will be at the expanse of more fuel consumption due to the increase in drag force.

سلامة السيارة واستقرارها هي واحدة من أساسيات صناعة السيارات. وهذا يؤخذ على محمل الجد. من أجل الحفاظ على سلامة الركاب وحياتهم. يرتبط استقرار السيارة بالديناميكا الهوائية للمركبة. بشكل عام عندما يتم تحسين الديناميكا الهوائية للمركبة ، سيتم تحسين الاستقرار. في هذا المشروع سيتم إضافة نفق تحت الجسم للمركبة. من أجل زيادة ثبات السيارة ، لتقليل احتمالية وقوع حوادث الانقلاب الذاتية، خاصة عند السرعات العالية. تم تصميم نموذج سيارة ثلاثية الأبعاد باستخدام برنامج ال سوليد ويرك . و سيتم تحليل هذه المسألة بأستخدام برنامج الانسسز. لتحديد خصائص الديناميكا الهوائية للمركبة مثل الضغط ، قوة السحب ، قوة الرفع ، معامل السحب ومعامل الرفع. الهدف من هذا المشروع هو زيادة استقرار السيارة عن طريق زيادة قوة الرفع السالبة بعد إضافة النفق السفلي. تم تحليل تأثير النفق السفلي على المركبة باستخدام برنامج الانسسز. وبسبب هذه التعديلات ، سيتم زيادة الاستقرار. ولكن هذه الزيادة في الاستقرار سوف تكون على حساب زيادة استهلاك الوقود بسبب الزيادة في قوة السحب .

List of Figures

List of Tables

Chapter one

Introduction

1.1 Introduction:

The automotive industry is one of the biggest industry sectors in the world. Due to its role in transportation from one place to another with minimal time and effort. This industry is developing rapidly. Despite the level of sophistication and technology that has reached it. But it still faces several challenges, in the field of vehicle safety and stability on the road. Vehicle stability is related to vehicle aerodynamic. When the vehicle aerodynamic improved, vehicle performance on the stability level, will improved in conjunction with it.

Rollover accidents occur due to vehicle instability. This type of accidents have a higher fatality rates than other types of vehicle collisions. There are three parameters that result a rollover if there a trouble on it, steering input, speed, and friction with the ground. These parameters can be controlled to avoid rollover accidents. The friction with ground can be increased by increasing down force on the vehicle. Down force is generated due to deferential pressure between the top and bottom of the vehicle. These force should be increased to decrease the risk of rollover accident. The reducing process can be done by reducing pressure under the vehicle, increased the pressure above the vehicle, or both. Reducing the pressure under the vehicle can be obtained by:

1. Minimize the distance between the car bottom and ground as much as possible.
2. Create tunnel in the underbody of vehicle.

Minimizing the distance between the car bottom and ground, would result in decreasing center of gravity height. Which is a measure that indicates the tendency of a vehicle to roll-over.

Adding tunnel under vehicle to reduce pressure. An example of these tunnels shown in figure (1.1). To obtain these results the tunnel is designed by using Bernoulli principle which states that an increase in the speed of a fluid occurs simultaneously with a decrease in pressure or a decrease in the fluid's potential energy.

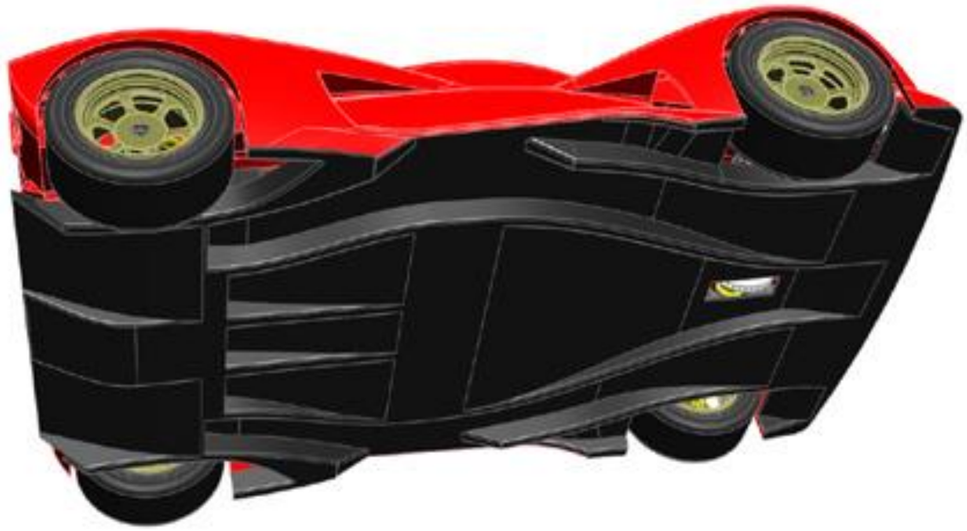

Figure 1.1 Example of car underbody tunnels

Increasing the pressure over the vehicle can be obtained by several methods. Adding rear wings, which helps primarily in acceleration, braking and cornering forces for the rear tires and combat oversteer.

To study the effect of these changes in aerodynamic. There are two ways, experimentally by wind tunnel test, or theoretically by simulation software's. Simulation method is preferred on experimental method. Because it is more accurate, lower cost and consumes much less time. Wind tunnel test takes three to four weeks, while more than 100 CFD simulation can performed.

1.2 Problem Definition:

Rollover accident happens as a result of vehicle instability especially at high speeds and in the case of cornering with high speed.

1.3 Project Objective:

The aim of this project is to improve vehicle aerodynamic. To obtain more stable vehicles. In order to avoid vehicle accidents.

1.4 Literature Review:

In these section three researches will be presented. Which have a link with vehicle aerodynamics and CFD simulation.

The first research aims to develop more fuel efficiency with lower emissions by reducing the drag resistance. The drag on the vehicle reduced, by reducing the differential pressure between the stagnation pressure on the front, and the bass pressure at the rear. And to obtain these reduction on drag resistance. A diffuser device was added on the vehicle underbody, and the underbody was modified to increase the base pressure. The analysis in the project just by using computational fluid dynamics simulation, without finding experimental data from the wind tunnel test, which has high cost and often takes place late in the development process which makes it hard to make any modification. And the results was The reduction in fuel consumption was small in low speeds, but when driving at high speeds the fuel consumption is lowered, because at higher speeds the aerodynamic drag force is the dominating resisting force and a reduction of 19% of the drag coefficient it will have a prominent effect on the fuel consumption when traveling in highways. [3]

The second research aims to reduce the drag of the car by modifying the car shape. . And the analysis of the aerodynamic characteristics by using ANSYS Fluent. The modification was change the angle of tailgate from 45 to 35. The object of this modification is to decrease the drag, increase the speed, decrease the fuel consumption, and decrease in damage over the structure. The simulation results shows a reduction in pressure and velocity distribution, and drag coefficient $C_d$which means a reduction in drag force. [6]

The third one aims to study the aerodynamic after adding rear wing and change the angle between the hood and windshield. The aerodynamic analysis was done by using the wind tunnel or computational fluid dynamics (CFD), CFD is a better solution due to the efficiency and the financial aspect**.** And the simulation results shows a maximum pressure locate at the top surface of the rear wing generating a down force in purpose of increasing traction and thus better acceleration at lower speed and less down force at higher speeds when the car is on straight line.[5]

1.5 Time Plan:

In this section the tasks and time tables will be determined as shown below:

Table 1.1 Task Description

Task ID	Task Description
T1	Drawing car model
T2	Case 1
T3	Case 2
T4	Case 3
T**5**	Case 4
T6	Writing the book

Table 1.2 Time plan

	1st semester														
Task/Week	1	2	3	4	5	6	7	8	9	10	11	12	13	14	15
T1															
T2															
T3															
T4															
T5															
T6															

Chapter Two

Vehicle Aerodynamic

2.1 Introduction:

Aerodynamic in general is the study of the motion of air, particularly its interaction with a solid object. It is a sub-field of fluid dynamics and gas dynamics, and many aspects of aerodynamics theory are common to these fields. In these chapter vehicle aerodynamics and fluid mechanics will be reviewed.

2.2 Fluid Mechanics:

As mentioned before aerodynamic is a sub-filed of fluid mechanics. In this section the history of aerodynamic sciences will be reviewed.

The early documentations were for the early scientist Archimedes (287_212 BC), who founded the fluid static filed, whose laws on buoyancy and flotation are used to this day. After then, the documentation of the famous Italian painter sculptor, Leonardo da Vinci (1452–1519). He was one of the first to document basic laws such as the conservation of mass. He sketched complex flow fields, suggested viable configuration for airplanes, parachutes, or even helicopters, and introduced the principle of streamlining to reduce drag. Then followed with a gradually developed in the next two hundred years, by the rational mathematical approach of Englishman, Sir Isaac Newton (1642–1727) to physics. A part from his basic laws of mechanics, and particularly the second law connecting acceleration with force, Newton developed the concept for drag and shear in a moving fluid, principles widely used today. [4]

Another famous scientists, Daniel Bernoulli (1700–1782). He pointed out the relation between velocity and pressure in a moving fluid, the equation of which bears his name in every textbook. [4]

This equation was formulated in the form known today, by his friend Leonhard Euler (1707–1783). In addition Euler, using Newton’s principles, developed the continuity and momentum equations for fluid flow. This equations are the basis for modern fluid dynamics and perhaps the most significant contribution in the process of understanding fluid flows. [4]

In the eighteenth century the foundations of fluid dynamics crystalized starting with Claude-Louis-Marie- Henri Navier (1785–1836), who understood that friction in a flowing fluid must be added to the force balance. He incorporated these terms into the Euler equations. After then the viscous term is added to the equation by Sir George Gabriel Stokes (1819–1903), to produce the final form of this equation which known today the Navier_Stokes equation. [4]

The Englishman Osborne Reynolds (1842–1912) came with important discoveries about turbulence and transition from laminar to turbulent flow. Ludwig Brandt (1874–1953), He made tremendous progress in developing simple models for problems such as boundary layers and airplane wings, and this leads us to the initial definition of aerodynamics. His assumptions usually considered low-speed airflow as incompressible. This assumption leading to significant simplifications. Considering in most cases the effects of viscosity were considered to be confined into a thin boundary layer, so that the viscous flow terms were neglected. These two major simplifications allowed the development of (aerodynamic) models that could be solved analytically and eventually compared well with experimental results. This trend of solving models and not the complex Navier–Stokes equations. [4]

2.2.1 Flow Classifications:

The flow of any fluid has some classifications such as; velocity pattern , change of density, statistically steady flow or unsteady and inviscid and viscous flow in this section these classifications will be reviewed .

2.2.1.1 Velocity Pattern: Turbulent, Laminar Flow:

To understand and compare between turbulent and laminar assuming a free-stream flow along the x-axis with uniform velocity U. following the traces made by several particles in the fluid it will expect to see parallel lines as shown in the upper part of Fig. 1.2. If, indeed, these lines are parallel and follow in the direction of the average velocity, and the motion of the fluid seems to be "well organized", then this flow is called laminar [1]. Then the velocity vector will be:

$$\vec{q} = (u, v, w) \qquad (2.1)$$

Then for this steady state flow the velocity vector will be:

$$\vec{q} = (U, 0,0) \qquad (2.2)$$

Where U is the velocity into the x direction, and q for the velocity vector.

Assuming in the second case have the same average speed (U_{av})in the flow, but in addition to this average speed the fluid particles will momentarily move into the other directions (lower part of Fig. 2.1). The fluid is then called turbulent. Assuming the average velocity for laminar and turbulence flow is the same. Also, in this two-dimensional case the flow is time dependent everywhere and average velocities into y and z directions are zero, the velocity vector then becomes:

$$\vec{q} = (U_{av} + u, v, w). \qquad (2.3)$$

$$\text{Where } V_{av} = W_{av} = 0 \qquad (2.4)$$

Where u, v, w are the perturbation into the x, y, and z directions.

Knowing whether the flow is laminar or turbulent is very important for most engineering problems since features such as friction and momentum exchange can change significantly between these two types of flow. The fluid flow can become turbulent in numerous situations such as inside long pipes or near the surface of high-speed vehicles [1].

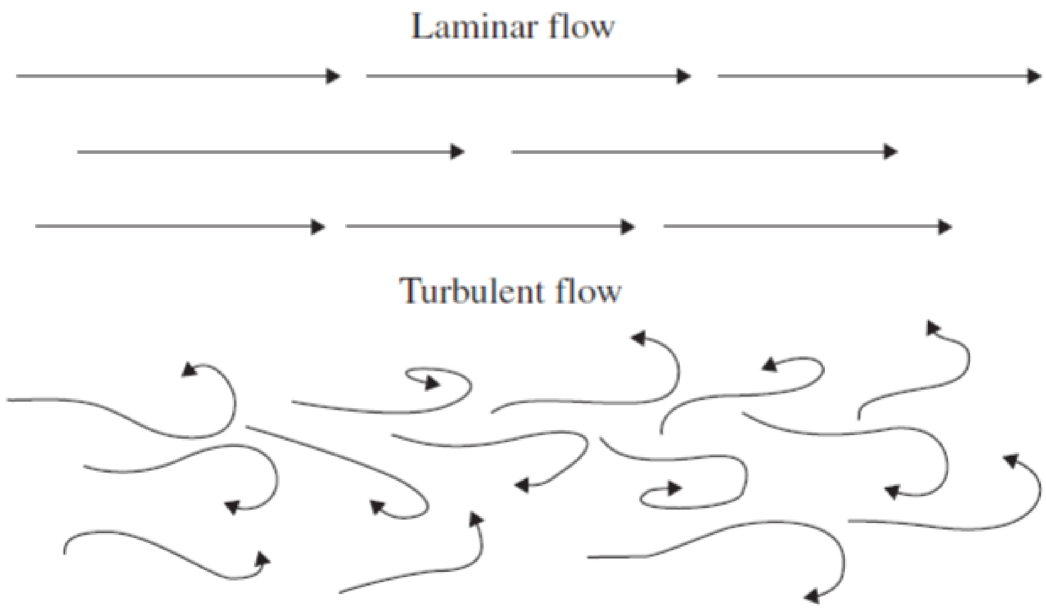

Figure 2.1 Schematic descriptions of laminar and turbulent flows with the same average velocity.

2.2.1.2 Change of Density: Incompressible, Compressible Flow:

Fluid density generally changes with pressure and temperature. For example taking the water. The change in density very small with pressure change, when the water in the liquid state. In contrast a significant change can be observed in the gaseous state [2].

In the case of statically steady flow of liquids substances with negligibly density change the flow is called incompressible flow. In gaseous state, he density change is a function of the flow Mach number. As shown in the figure 2.2, which represents the relative changes of different flow properties as functions of the flow Mach number [2].

Meaning that the flow may be considered incompressible. When Mach number $M > 0.3$ density changes cannot be neglected and the flow considered as compressible flow. Mach number gives a practical idea about the density change. A more adequate definition whether the flow can be considered compressible or incompressible is given by the condition $D\rho/Dt = 0$ [2].

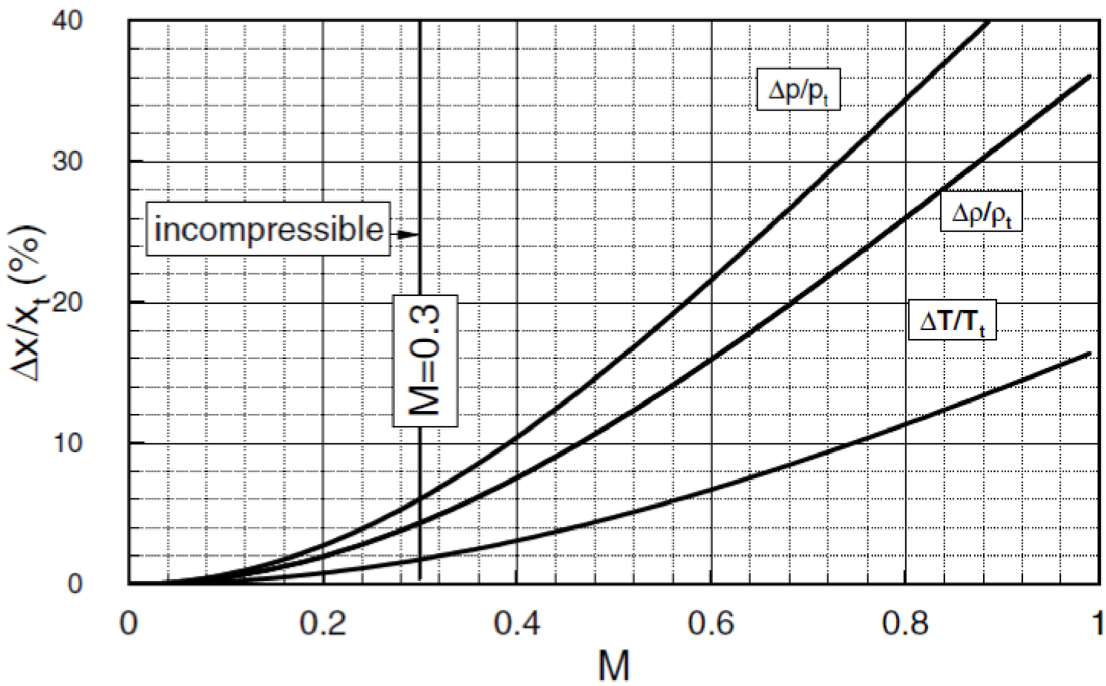

Figure 2.2 Density, pressure, and temperature changes as a function of the flow Mach number

Up to $M = 0.3$ the relative changes of density may be considered negligibly small

2.2.1.3 Statistically Steady Flow, Unsteady Flow:

Figure 2.3 illustrates the nature of the statistically steady and unsteady flow types. As an example, Fig. 2.3(a) shows the velocity distribution of a statistically steady turbulent pipe flow with a constant mean. Fig. 2.3(b) represents the turbulent velocity of a statistically unsteady flow discharging from a container under pressure. As seen, the mean velocity is a function of time. A periodic unsteady turbulent flow through a reciprocating engine is represented by Fig. 2.3(c) [2].

In Figure 2.3, random fluctuations typical of a turbulent flow are superimposed on the mean flow. For steady or unsteady laminar flows where the Reynolds number is below the critical one, the velocity distributions do not have random component as shown in Fig. 2.4[2].

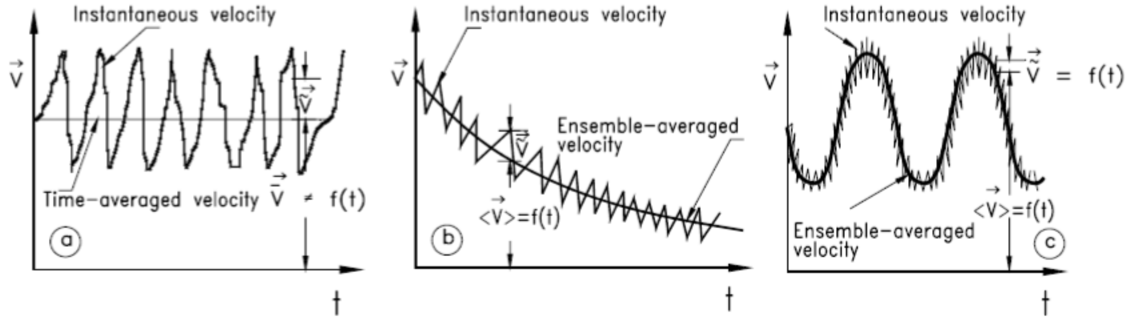

Figure 2.3 Statistically steady and unsteady turbulent flows.

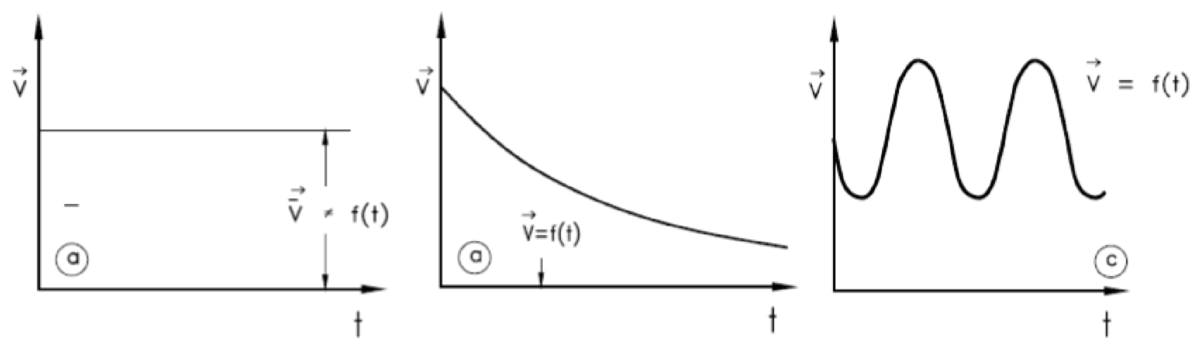

Figure 2.4 Steady and unsteady laminar flows.

2.2.1.4 Inviscid and Viscous Flow:

The ability of fluid molecules to move freely. When the molecules move, even in a very random fashion, they obviously transport their mass, momentum, and energy from one location to another in the fluid. This transport on a molecular scale gives rise to the phenomena of mass diffusion, viscosity (friction), and thermal conduction. This transport phenomena found in.

2.2.2 Visualization of Fluid Flow:

The quantitative and qualitative information of fluid flow can be obtained through sketches, photographs, graphical representation and mathematical analysis. However, the visual representation of flow fields is very important in modeling the flow phenomena. There is three sets of curves describes the fluid motion such as; pathline, streakline, and streamline[1].

2.2.2.1 Pathlines:

Pathline or a particle path is a curve describing the trajectory of a fluid element .Pathlines are obtained in the Lagrangian approach by an integration of the equations of dynamics for each fluid particle. And can be produced in the laboratory by marking the fluid particle and taking time exposure photograph of its motion [1].

2.2.2.2 Streakline:

In many cases of experimental flow visualization, particles are introduced into the flow at a fixed point in space. The line connecting all of these particles is called a streak line. Here, the attention is focused to a fixed point in space (i.e. Eulerian approach) and identifying all fluid particles passing through that point. These lines are laboratory tool rather than analytical tool. They are obtained by taking instantaneous photographs of selected particles that have passed through a given location in the flow field [1].

2.2.2.3 Streamline:

These are the lines drawn in the flow field so that at a given instant, they are tangent to the direction of flow at every point in the flow field. Mathematically, these lines are obtained analytically by integrating the equations defining lines tangent to the velocity field. In a two dimensional flow field as shown in the figure 2.5, the slope of the streamline is equal to the tangent of the angle that velocity vector makes with x-axis as shown in the figure:

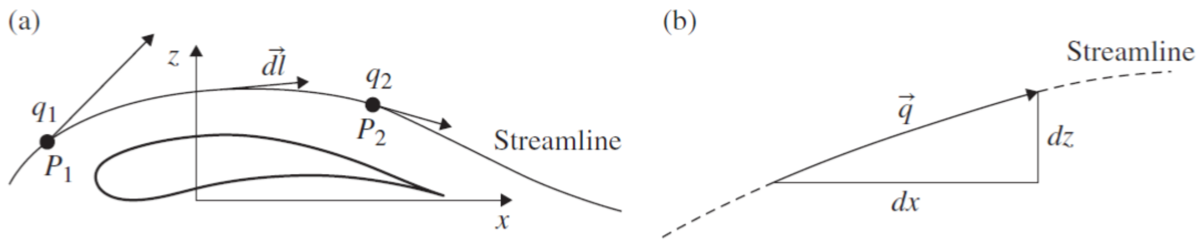

Figure 2.5 Streamlines definition.

Where q the tangent velocity vector, l the streamline .When q is tangent to the streamline dl therefore:

$$\vec{q}.\vec{dl} = 0 \qquad (2.5)$$

If the velocity vector is $\vec{q} = (u, v, w)$, then the vector equation (Eq. 2.5) reduces to the following scalar equations:

$$\begin{aligned} wdy - vdz &= 0 \\ udz - wdx &= 0 \\ vdx - udy &= 0 \end{aligned} \qquad (2.6)$$

In a differential equation form:

$$\frac{dx}{u} = \frac{dy}{v} = \frac{dz}{w} \qquad (2.7)$$

The velocity components in the $x - z$ plane are $\vec{q} = (u, w)$ and the slope of the streamline is dz/dx , which is equal to the slope of the velocity vector:

$$\frac{dz}{dx} = \frac{w}{u} \qquad (2.8)$$

2.2.3 Attached and Separated Flow:

When the streamlines near the solid surface follow exactly the shape of the body (as in Fig. 2.6a) the flow is considered to be attached. If the flow does not follow the shape of the surface (as seen behind the vehicle in Fig. 2.6b) then the flow is considered to be separated. Usually, such separated flows behind the vehicle will result in an unsteady wake flow, which can be felt up to large distances behind it [1].

Having attached flow fields is extremely important because vehicles with larger areas of flow separation are likely to generate higher resistance (drag).

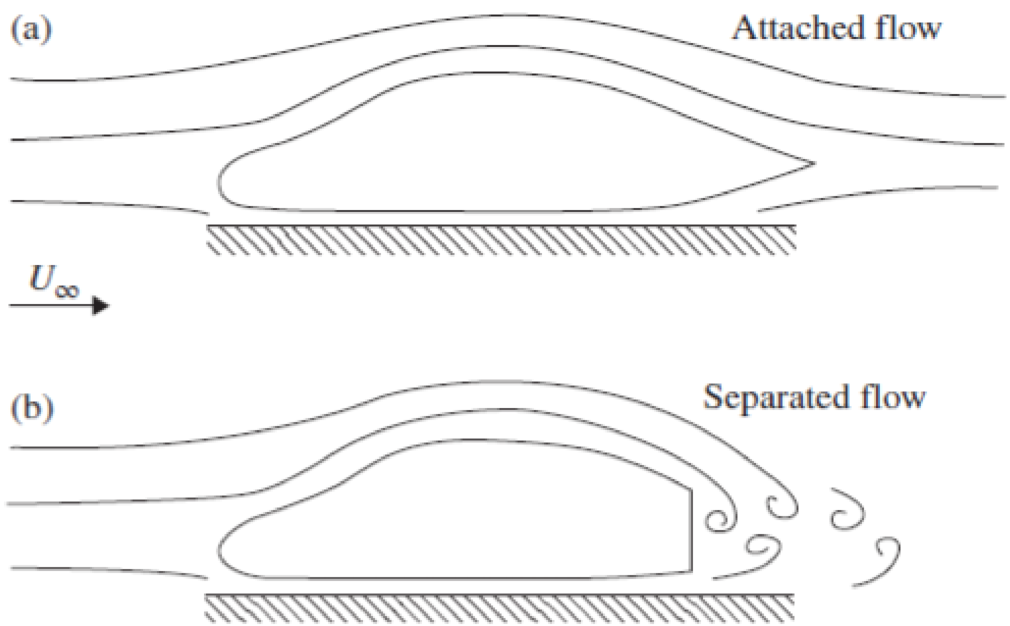

Figure 2.6 Attached flow over a streamlined car (a) and the locally separated flow behind a more realistic automobile shape (b)

2.2.4 Fluid Properties:

2.2.4.1 Density:

In case of fluids the density defined as the limit of mass per unit volume. When a measuring volume V is shrinks to zero. We need to use this definition since density can change from one point to the other [1].

Therefore, the definition of density at a specific point is:

$$\rho = \lim_{v \to 0} \left(\frac{m}{V} \right) \qquad (2.9)$$

2.2.4.2 Pressure:

The pressure p as the limit of the normal force F, per unit area, acting on a surface S. we use the limit process to define pressure at a point, since it may vary on a surface [1].

$$\text{p} = \lim_{S \to 0} \left(\frac{F}{S} \right) \qquad (2.10)$$

Bernoulli pictured the pressure to be a result of molecules impinging on a surface. The fluid pressure acting on a solid surface is normal to the surface[1].

The direction is obtained by multiplying with the unit vector n normal to the surface. Thus, the pressure acts normal to a surface, and the resulting force, ΔF is:

$$\Delta F = -P\vec{n}\ \text{dS} \qquad (2.11)$$

The minus sign is a result of the normal unit-vector pointing outside the surface while the force due to pressure points inward. Also note that the pressure at a point inside a fluid is the same in all directions. This property of the pressure is called isetropic [1].

2.2.4.3 Temperature:

The temperature is a measure of the internal energy at a point in the fluid [1].

2.2.4.4 Viscosity:

The viscosity is a very important property of fluids, particularly when fluid motion is discussed. A fluid must be in motion in order to generate a shear force, while a solid can support shear forces in a stationary condition [1].

2.2.5 The Laminar Boundary Layer:

From the historical perspective, the German Scientist Ludwig Prandtl (1874–1953) was the first to develop the two-dimensional boundary-layer equations, almost 1904. One of his first students, Paul Richard Heinrich Blasius (1883–1970) provided the first analytical solution (1908) for these equations [1].

Boundary layer is the region near a solid surface the fluid particles must adhere to the zero slip boundary condition and therefore viscous effects cannot be neglected. We will discuss viscous effects, in spite of the "high Reynolds number flow" assumption [1].

As the air moves around the body, its velocity changes and at any point we can call this (outer) velocity Ue. Within the thin boundary layer, its thickness denoted as δ, the velocity must change from zero on the solid surface to Ue,. Which is shown in figure 2.7[1].

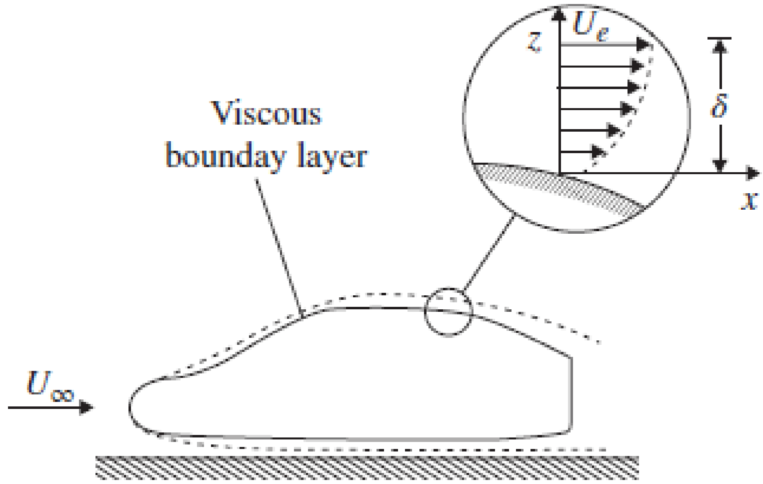

Figure 2.7 Schematic description of a high Reynolds number flow boundary layer on the upper surface of a car. The inset depicts the velocity distribution near the solid surface.

Basic boundary layer model and the elements necessary to explain the concept of combining the inner viscous and the outer in viscid flows. With these two (inner and outer) high Reynolds number flow models in mind, the information sought from the viscous boundary layer solution in this chapter is:

1. The scale, or thickness, of the boundary layer and its streamwise growth.

2. Displacement effects (to the outer flow model) due to the slower velocity inside the viscous layer.

3. The skin-friction and resulting drag estimates that cannot be calculated by the outer inviscid flow.

4. Based on the laminar boundary layer model, parameters such as the boundary layer thickness or the skin friction will be extended into the turbulent flow range, mostly using empirical correlations.

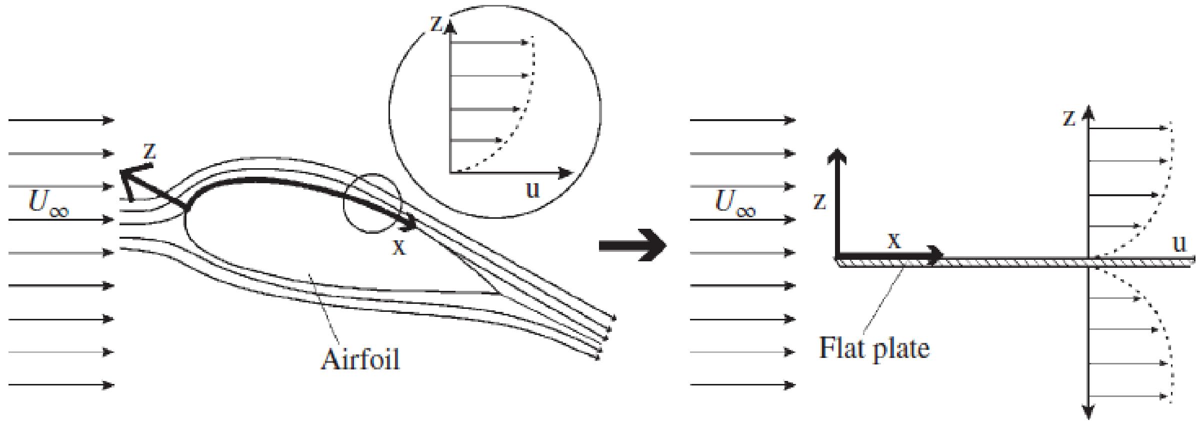

Figure 2.8 Similarity of the boundary layer developing on a curved surface to the proposed flatplate model.

The figure 2.8 show Similarity of the boundary layer developing on a curved surface to the proposed flatplate model shows that for moderately curved surfaces the above approximation is accurate to the first order and even for second order approximation, the correction is small. Therefore, we shall proceed with the simple flat plate model and assume that for attached flows this model can reasonably estimate the expected boundary layer properties [1].

The equation for boundary layer is:

$$\frac{\partial}{\partial t}\int_0^{\delta} u dz + \frac{d}{dx}\int_0^{\delta} u^2 dz - U_e \frac{d}{dx}\int_0^{\delta} u dz = -\frac{\tau_w}{\rho} - \frac{1}{\rho}\frac{d\rho}{dx}\delta \qquad (2.12)$$

This equation is named after the Hungarian born and later US scientist Theodore von Kármán (1881–1963) who completed his Doctoral dissertation u nder Prandtl.

2.3 Vehicle Aerodynamic:

Our cars simply is not designed to go through a brick wall. But there is another type of wall that cars designed to move through, the wall of air that pushes against a vehicle at high speeds. At low speeds and the air is quite. It's hard to notice the air wall and the way that interacts with our vehicle. Which is appears at high speeds. Air interactions with moving objects create forces acted upon this object this called air resistance or drag force. This resistance affects the way a car accelerates, handles and achieves fuel mileage.

Here the science of aerodynamics comes into play. Vehicle aerodynamic is defined as the study of the aerodynamics of road vehicles. Its main goals are reducing drag and wind noise, minimizing noise emission, and preventing undesired lift forces and other causes of aerodynamic instability at high speeds.

Aerodynamics has a positive sides such as it helps in ventilation, in-and-out flows and brake cooling. On the other hand, there is a negative side which is resulting forces on the vehicle. The forces are drag (force resist the motion), the tire rolling resistance and driveline friction effects. This forces resist the motion of the vehicle. So it must overcome this forces to drive the car from stand still. The effects of these forces shown on figure (2.9) [1].

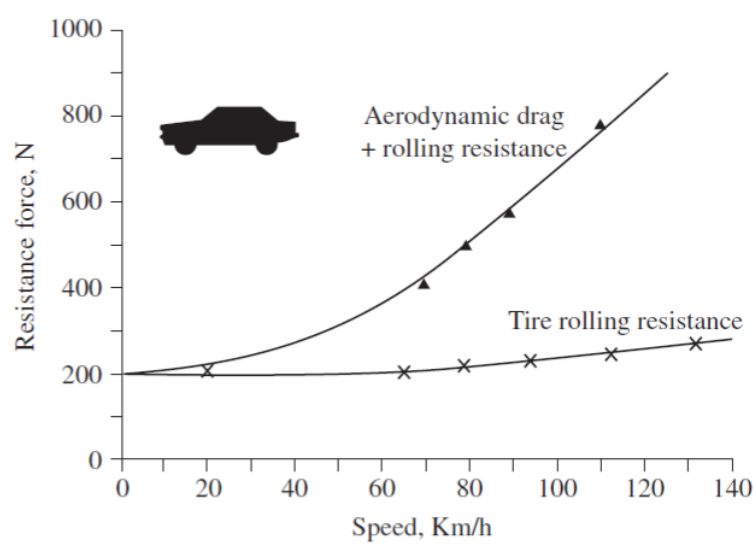

Figure 2.9 Increase of vehicle total drag and tires rolling resistance on a horizontal surface, versus speed.

The test shown in this figure that the aerodynamic drag increases with the square of velocity. While all other components of drag change only marginally [1].

2.3.1 History of Aerodynamic:

There’s a rich design history between the strictly utilitarian designs of the early 20th century and the double-take inducing designs of modern day, and like many forms of progress it has come in fits and starts.

The development of the cars aerodynamics at the last century was develop from a drag coefficient around 2.1 to a drag coefficient (0.3 _0.18). As shown in figure (2.10).

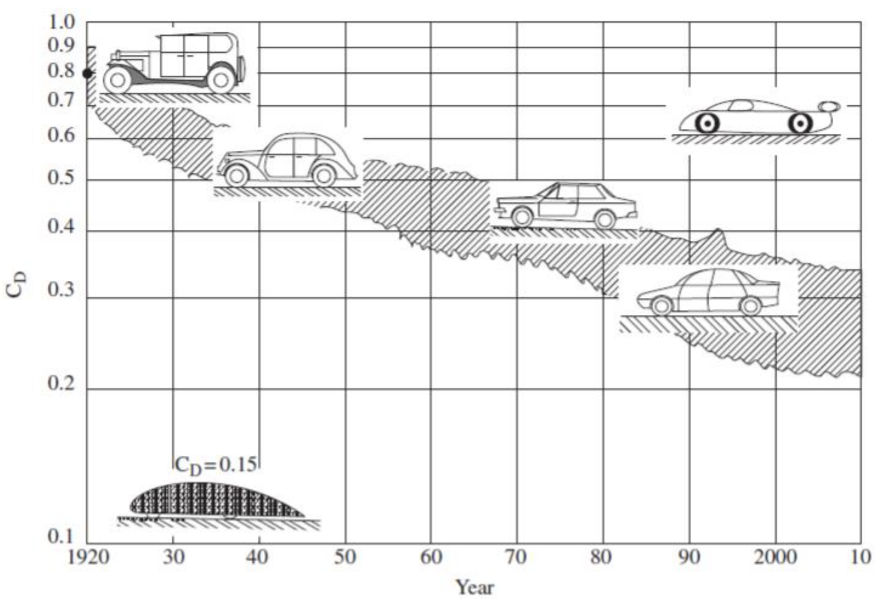

Figure 2.10. Drag coefficient development history.

There’s a rich design history between the strictly utilitarian designs of the early 20th century and the double-take inducing designs of modern day, and like many forms of progress it has come in fits and starts.

There was nothing aerodynamics about the earliest cars. For example take a look at Ford's seminal Model T it looks more like a horse carriage. a very boxy design, indeed. Many of these early cars didn't need to worry about aerodynamics because they were relatively slow. However, some racing cars of the early 1900s incorporated tapering and aerodynamic features to one degree or another.

In 1921, German inventor Edmund Rumpler created the Rumpler-Tropfenauto, which translates into "tear-drop car." Based on the most aerodynamic shape in nature, the teardrop, it had a Cd of just 0.27.

On the American side, one of the biggest leaps ahead in aerodynamic design came in the 1930s with the Chrysler Airflow. Inspired by birds in flight, the Airflow was one of the first cars designed with aerodynamics in mind.

Though it used some unique construction techniques and had a nearly 50-50-weight distribution (equal weight distribution between the front and rear axles for improved handling), a Great Depression-weary public never fell in love with its unconventional looks, and the car was considered a flop. Still, its streamlined design was far ahead of its time.

As the 1950s and '60s came about, some of the biggest advancements in automobile aerodynamics came from racing. Originally, engineers experimented with different designs, knowing that streamlined shapes could help their cars go faster and handle better at high speeds. That eventually evolved into a very precise science of crafting the most aerodynamic race car possible. Front and rear spoilers, shovel-shaped noses, and aero kits became more and more common to keep air flowing over the top of the car and to create necessary downforce on the front and rear wheels.

On the consumer side, companies like Lotus, Citroën and Porsche developed some very streamlined designs, but these were mostly applied to high-performance sports cars and not everyday vehicles for the common driver. That began to change in the 1980s with the Audi 100, a passenger sedan with a then-unheard-of Cd of .30. Today, nearly all cars are designed with aerodynamics in mind in some way.

2.3.2 Aerodynamic Force:

With growing emphasis on fuel economy and on the reduction of undesirable exhaust emissions, it has become increasingly important to optimize vehicle power requirements. To achieve this, it is necessary to reduce the aerodynamic resistance, rolling resistance, and inertia resistance, which is proportional to vehicle weight.

The aerodynamic resistance is generated by two sources: one is the airflow over the exterior of the vehicle body, and the other is the flow through the engine radiator system and the interior of the vehicle for purposes of cooling, heating, and ventilating.

There are three aerodynamic forces drag force, lift force and down force, will be explained in this section.

2.3.2.1 Drag Force:

Aerodynamic drag is a turbulent losses occur in some areas due to air flow around the vehicle. The largest contribution comes from the vortex behind the car (Figure 2.11). Small vortices at wheels, mirrors, and the engine compartment and at the A-column (Figures 2.12 and 2.13) contribute to the aerodynamic drag, too. The force exerted by the formation of these vortices on the vehicle is:

$$F_a = \frac{1}{2} c_d A \rho_a v_r^2 \qquad (2.13)$$

Where c_d is the drag coefficient, A is the frontal area, ρ_a the density of the air, and v_r is the air velocity. This resulting velocity comes from the driving velocity of the vehicle, v_v, and wind velocity, v_a.

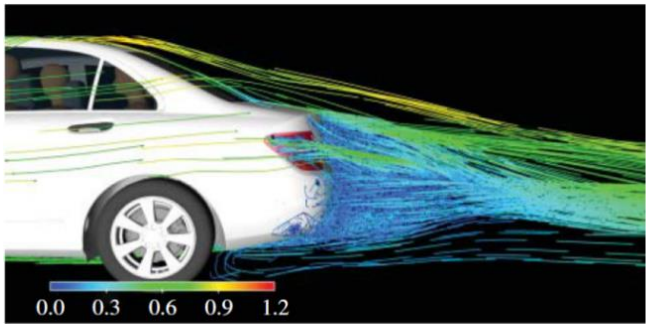

Figure 2.11 Vortex behind a car (reproduced with permissions of Daimler AG).

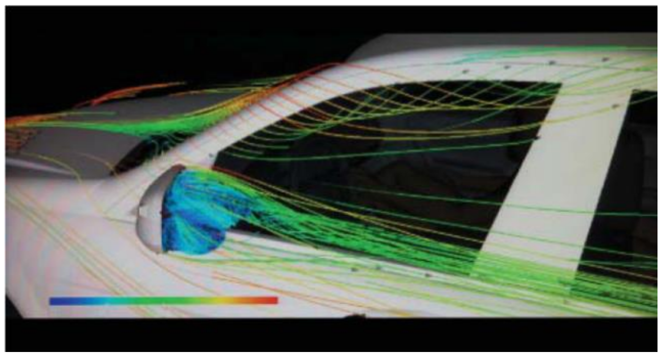

Figure 2.12 Vortex at A-column (reproduced with permissions of Daimler AG).

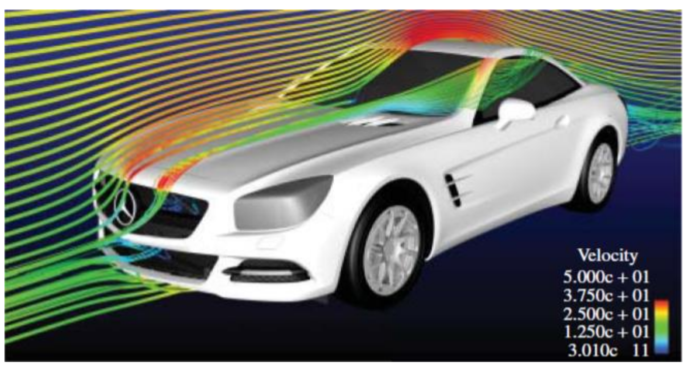

Figure 2.13 Vortex at engine compartment and at A-column (reproduced with permissions of Daimler AG).

The drag coefficient depends on the low direction. In order to achieve a better comparison of vehicles, it is common to use a simplified approach in which the wind speed is not considered.

Aerodynamic drag force: On a vehicle with the projected frontal area, A, travelling at a speed $v_v$in the longitudinal direction, a longitudinal force F_a, the so-called aerodynamic drag force, acts as follows (wind velocity v_a= 0):

$$F_a = \frac{1}{2} C_d A \rho_a v_v^2 \qquad (2.14)$$

Here cd is the coefficient of aerodynamic drag. The value of c_d for modern passenger cars is about 0.2–0.3. A typical size for the frontal area A is $2m^2$.

2.3.2.2 Lift Force:

Aerodynamic lift acting on a vehicle is caused by the pressure differential across the vehicle body from the bottom to the top. It may become significant at moderate speeds. The aerodynamic lift usually causes the reduction of the normal load on the tire-ground contact [3].

The aerodynamic lift R_L, acting on a vehicle is usually expressed by:

$$F_l = \frac{1}{2} C_l A \rho_a v_v^2 \ . \qquad (2.15)$$

Where C_L is the coefficient of aerodynamic lift.

2.3.2.3 Down Force:

Aerodynamic downforce the same principles which allow aircraft to fly are similar in racecar aerodynamics, but the main focus is to produce downforce instead of negative lift.

There are many benefits of using downforce, it will preserve its tires and reduce their heating and wear due to friction (slip), turns the vehicle faster or braking harder when longitudinal slip is considered, improve vehicle stability, and can result in shorter braking distances and faster exits from turns [1].

These force created by the aerodynamic characteristics of a car that allows it to travel faster through a corner by holding the car to the track or road surface. Some elements to increase vehicle downforce will also increase drag. It is very important to produce a good downward aerodynamic force because it affects the car’s speed and traction.

We can create an aerodynamic downforce (reduce the lift) by two ways:

1. The first way is to use the shape of the vehicle and its usually requires the contouring of the underbody, like:
   a. Ground effect.
   b. Rear diffuser “Venturi”.
   c. Underbody tunnels (combination of the previous two).
   d. Vacuum cleaner: Sealing the whole lower part of the vehicle and creating low pressure by suction.

2. The second way is by adding negative lifting devices such as:
   a. Inverted Wings
   b. Splitter plates
   c. Dive plates
   d. Louvers
   e. Vortex generators.

2.4 Vehicle Handling and Stability:

In recent years, aerodynamics have become an area of increasing focus by racing teams as well as car manufacturers. Advanced tools such as wind tunnels and computational fluid dynamics (CFD) have allowed engineers to optimize the handling characteristics of vehicles.

Car designers often bias the car's handling toward less corner-entry understeer (such as by lowering the front roll center), and add rearward bias to the aerodynamic downforce to compensate in higher-speed corners. The rearward aerodynamic bias may be achieved by an airfoil or "spoiler" mounted near the rear of the car, but a useful effect can also be achieved by careful shaping of the body as a whole, particularly the aft areas.

Vehicle handling is defined as the descriptions of the way a wheeled vehicle responds and reacts to the inputs of a driver, as well as how it moves along a track or road. It is commonly judged by how a vehicle performs particularly during cornering, acceleration, and braking as well as on the vehicle's directional stability when moving in steady state condition.

2.4.1 Center of Mass Height:

The center of mass height, relative to the track, determines load transfer (related to, but not exactly weight transfer) from side to side and causes body lean. When tires of a vehicle provide a centripetal force to pull it around a turn, the momentum of the vehicle actuates load transfer in a direction going from the vehicle's current position to a point on a path tangent to the vehicle's path. This load transfer presents itself in the form of body lean. In extreme circumstances, the vehicle may roll over.

Height of the center of mass relative to the wheelbase determines load transfer between front and rear. The car's momentum acts at its center of mass to tilt the car forward or backward, respectively during braking and acceleration. Since it is only the downward force that changes and not the location of the center of mass, the effect on over/under steer is opposite to that of an actual change in the center of mass. When a car is braking, the downward load on the front tires increases and that on the rear decreases, with corresponding change in their ability to take sideways load.

A lower center of mass is a principal performance advantage of sports cars, compared to sedans and (especially) SUVs. Some cars have body panels made of lightweight materials partly for this reason.

2.4.2 Center of Mass:

In steady-state cornering, front-heavy cars tend to understeer and rear-heavy cars to oversteer (Understeer & Oversteer explained), all other things being equal. The mid-engine design seeks to achieve the ideal center of mass, though front-engine design has the advantage of permitting a more practical engine-passenger-baggage layout. All other parameters being equal, at the hands of an expert driver a neutrally balanced mid-engine car can corner faster, but a FR (front-engine, rear-wheel drive) layout car is easier to drive at the limit.

The rearward weight bias preferred by sports and racing cars results from handling effects during the transition from straight-ahead to cornering. During corner entry the front tires, in addition to generating part of the lateral force required to accelerate the car's center of mass into the turn, also generate a torque about the car's vertical axis that starts the car rotating into the turn. However, the lateral force being generated by the rear tires is acting in the opposite torsional sense, trying to rotate the car out of the turn. For this reason, a car with "50/50" weight distribution will understeer on initial corner entry. To avoid this problem, sports and racing cars often have a more rearward weight distribution. In the case of pure racing cars, this is typically between "40/60" and "35/65".[*citation needed*] This gives the front tires an advantage in overcoming the car's moment of inertia (yaw angular inertia), thus reducing corner-entry understeer.

Using wheels and tires of different sizes (proportional to the weight carried by each end) is a lever automakers can use to fine tune the resulting over/understeer characteristics.

2.4.3 Roll Angular Inertia:

This increases the time it takes to settle down and follow the steering. It depends on the (square of the) height and width, and (for a uniform mass distribution) can be approximately calculated by the equation:

$$I = M(H^2 + W^2) \ . \qquad (2.16)$$

Greater width, then, though it counteracts center of gravity height, hurts handling by increasing angular inertia. Some high performance cars have light materials in their fenders and roofs partly for this reason

2.4.4 Yaw and pitch angular inertia:

Unless the vehicle is very short, compared to its height or width, these are about equal. Angular inertia determines the rotational inertia of an object for a given rate of rotation. The yaw angular inertia tends to keep the direction the car is pointing changing at a constant rate.

This makes it slower to swerve or go into a tight curve, and it also makes it slower to turn straight again. The pitch angular inertia detracts from the ability of the suspension to keep front and back tire loadings constant on uneven surfaces and therefore contributes to bump steer. Angular inertia is an integral over the square of the distance from the center of gravity, so it favors small cars even though the lever arms (wheelbase and track) also increase with scale. (Since cars have reasonable symmetrical shapes, the off-diagonal terms of the angular inertia tensor can usually be ignored.) Mass near the ends of a car can be avoided, without re-designing it to be shorter, by the use of light materials for bumpers and fenders or by deleting them entirely. If most of the weight is in the middle of the car then the vehicle will be easier to spin, and therefore will react quicker to a turn.

2.4.5 Rollover:

These type of accidents in which the vehicle tips over onto its side or roof. And have a higher fatality rate than other types of vehicle collisions.

Vehicle rollovers are divided into two categories: tripped and untripped. Tripped rollovers are caused by forces from an external object, such as a curb or a collision with another vehicle. Untripped crashes are the result of steering input, speed, and friction with the ground

Untripped rollovers occur when cornering forces destabilize the vehicle. As a vehicle rounds a corner, three forces act on it: tire forces (the centripetal force), inertial effects (the centrifugal force), and gravity. The cornering forces from the tire push the vehicle towards the center of the curve. This force acts at ground level, below the center of mass. The force of inertia acts horizontally through the vehicle's center of mass away from the center of the turn. These two forces make the vehicle roll towards the outside of the curve. The force of the vehicle's weight acts downward through the center of mass in the opposite direction. When the tire and inertial forces are enough to overcome the force of gravity, the vehicle starts to turn over.

Chapter Three
Computational Fluid Dynamics

3.1 Introduction:

Computational fluid dynamics is a simulation tool that uses numerical analysis, applied physics and computational software to visualize how a fluid flows. The process is as shown in figure (3.1).

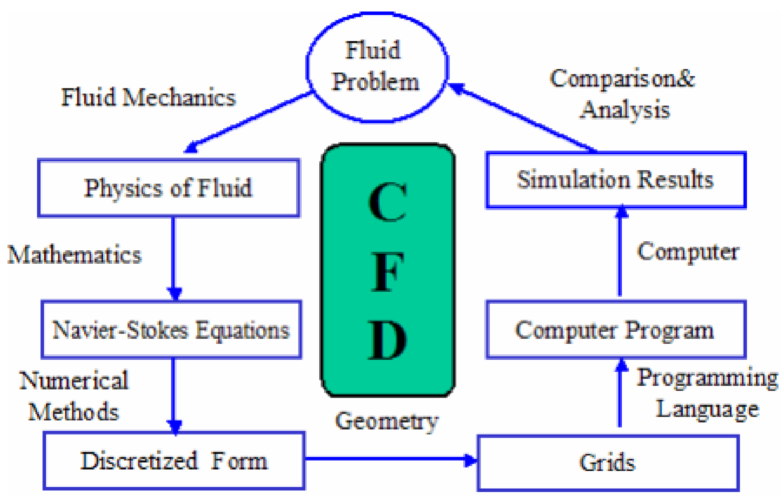

Figure 3.1 CFD process

Firstly, we have a fluid problem. To solve this problem, the physical properties of fluid should be known by using Fluid Mechanics. Then the mathematical equations will be used to describe these physical properties. This is Navier-Stokes Equation and it is the governing equation of CFD, which will be discussed latter in this chapter.

3.2 CFD softwares:

There is a lot of CFD softwares, some of them specialized just in CFD simulation, for example ANSYS, and the other not specialized. CFD simulation is one of its multiple function. For example MATLAB and Solidworks.

3.2.1 MATLAB:

It a multi-paradigm numerical computing environment. A proprietary programming language developed by Math Works, MATLAB allows matrix manipulations, plotting of functions and data, implementation of algorithms, creation of user interfaces, and interfacing with programs written in other languages, including C, C++, C#, Java, Fortran and Python.

3.2.2 SOLIDWORKS:

A three-dimensional mechanical design application (CAD). This program works under the Microsoft Windows environment developed by the company Dassault Systèmes SolidWorks Corp.

3.2.3 ANSYS:

ANSYS software is used to design products and semiconductors, as well as to create simulations that test a product's durability, temperature distribution, fluid movements, and electromagnetic properties.

3.3 Strategy of CFD:

The strategy of CFD is by replacing the continuous problem domain with a discrete domain using a grid. In the continuous domain each flow variable is defined at every point in the domain, but in the discrete domain, each flow variable is defined only at the grid points and the values at other locations are determined by interpolating the values at the grid points.

Domain is discretized into a finite set of control volume or cells. The discretized domain is called the "grid" or the "mesh." On other words we discretize second order differential equation into algebraic equations.

3.4 Navier_Stokes Equations:

The Navier-Stokes equations are the basic governing equations for a viscous, heat conducting fluid. It is a vector equation obtained by applying Newton's Law of Motion to a fluid element and is also called the momentum equation. It is supplemented by the mass conservation equation, also called continuity equation and the energy equation. Usually, the term Navier-Stokes equations is used to refer to all of these equations. The Navier-Stokes equation is named after Claude-Louis Navier and George Gabriel Stokes.

3.4.1 Derivation of Navier_Stokes Equations:

3.4.1.1 Eulerian and Lagrangian Description of Conservation Laws:

Eulerian (control volume) approach: focuses on specific locations in the flow regions as time passes. As shown in figure 3.2(a).

Lagrangian (material volume) approach: subdivide fluid into fluid particles and every particle is followed as it moves through space and time. As shown in figure 3.2(b).

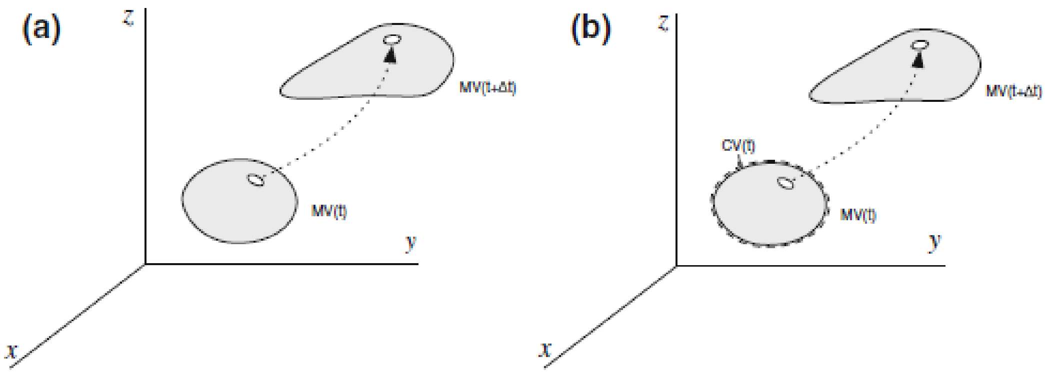

Figure 3.2 (a) Lagrangian and (b) Eulerian specification of the flow field.

Euler derivative ($d\phi / dt$): the derivative of a filed variable ϕ (t,x(t))with respect to a fixed position in space. Lagrange derivative ($D\phi / Dt$): The derivative following a moving fluid particle [4].

$$\frac{D\phi}{Dt} = \frac{\partial\phi}{\partial t}\frac{dt}{dt} + \frac{\partial\phi}{\partial x}\frac{dx}{dt} + \frac{\partial\phi}{\partial y}\frac{dy}{dt} + \frac{\partial\phi}{\partial z}\frac{dz}{dt} \quad (3.1)$$

$$= \frac{\partial\phi}{\partial t} + u\frac{\partial\phi}{\partial x} + v\frac{\partial\phi}{\partial y} + w\frac{\partial\phi}{\partial z} \quad (3.2)$$

$$= \frac{\partial\phi}{\partial t} + v.\nabla\phi \quad (3.3)$$

3.4.1.2 Reynolds Number:

The Reynolds number is the ratio of inertial forces to viscous forces within a fluid which is subjected to relative internal movement due to different fluid velocities, in which is known as a boundary layer in the case of a bounding surface such as the interior of a pipe.

The Reynolds number (Re) is defined as:

$$\mathrm{Re} = \frac{\rho U L}{\mu} \qquad (3.4)$$

Where ρ the density of the fluid is, U is the velocity of the fluid (m/s), L is a characteristic linear dimension (m), and μ is the dynamic viscosity of the fluid.

And may be interpreted as a measure of the relative importance of advection (inertia) to diffusion (viscous) momentum fluxes. If the momentum fluxes are in the same direction then the Reynolds number reveals the boundary layer characteristics of the flow. If the fluxes are defined such that the diffusion is in the cross stream direction, then as shown in Fig.(3.3) Re conveys the flow regime (i.e. laminar, transitional, or turbulent).

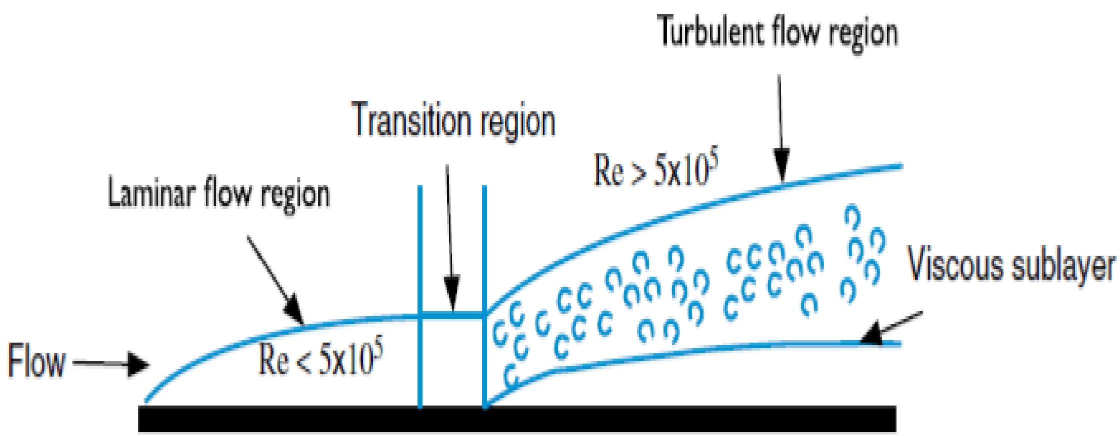

Figure 3.3 Laminar, transitional, or turbulent.

An example showing the flow field for different values of Reynolds number is depicted in Fig. (3.4).

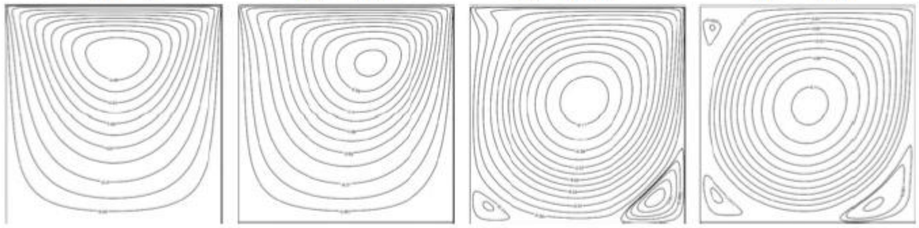

Figure 3.3 Flow field for different values of Reynolds number.

3.4.1.3 Reynolds Transport Theorem:

Conservation laws apply to a moving material volumes of fluids, and not to fixed point or control volumes. We want to express these laws following an eulerian approach because in lagrangian approach there is no ability to control the domain of interest since fluid particle travel to where the flow takes them which may not to be the region of interest [4].

Reynolds transport theorem:

$$\left(\frac{dB}{dt}\right)_{MV} = \frac{d}{dt}\left(\int_{V(t)} b\rho dV\right) + \int_{S(t)} b\rho v_r .ndS \tag{3.5}$$

3.4.1.4 Conservation of Mass:

The principle of conservation of mass indicates that in the absence of mass sources and sinks, a region will conserve its mass on a local level.

Derivation of continuity equation:

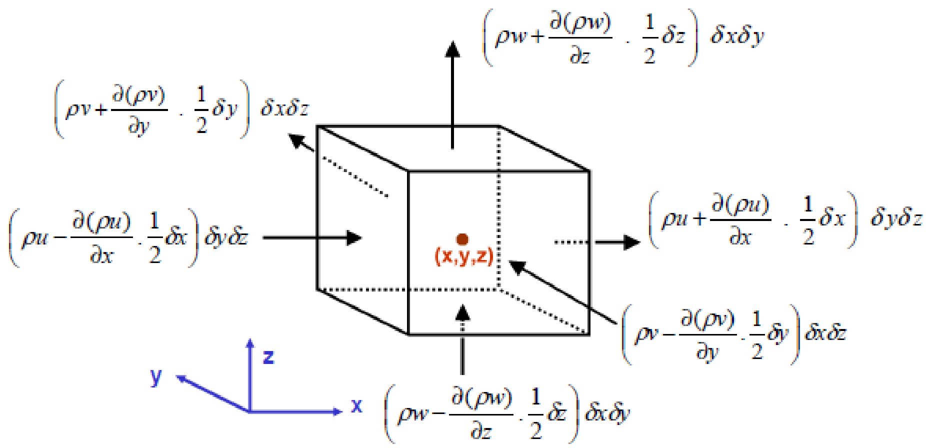

Figure 3.5 Fluid element.

The Change in the mass of the system equals the change in the control volume plus the mass in and mass out as shown in figure (3.5):

$$\frac{D_{m_{system}}}{Dt} = \frac{\partial m_{cv}}{\partial t} + \sum \dot{m}_{out} + \sum \dot{m}_{in} \tag{3.6}$$

The mass out from the $x-$ direction:

$$\left(\dot{m}_{out}\right)_x = \dot{m}_x + \frac{\partial \dot{m}_x}{\partial t} d_x \tag{3.7}$$

The mass out from the $y-$ direction:

$$\left(\dot{m}_{out}\right)_y = \dot{m}_y + \frac{\partial \dot{m}_y}{\partial t} d_y \tag{3.8}$$

The mass out from the $z-$ direction:

$$\left(\dot{m}_{out}\right)_z = \dot{m}_z + \frac{\partial \dot{m}_z}{\partial t} d_z \tag{3.9}$$

The equation (3.5) become:

$$= \frac{\partial \dot{m}_{cv}}{\partial t} + \dot{m}_x + \frac{\partial \dot{m}_x}{\partial x} dx + \dot{m}_y + \frac{\partial \dot{m}_y}{\partial y} dy + \dot{m}_z + \frac{\partial \dot{m}_z}{\partial z} dz - (\dot{m}_x + \dot{m}_y + \dot{m}_z) \tag{3.10}$$

Where:

$$m = \rho V = \rho dxdydz\,. \tag{3.11}$$

Substitute this term in the equation (3.10):

$$= \frac{\partial \rho}{\partial t} dxdydz + \frac{\partial \rho u}{\partial x} dxdydz + \frac{\partial \rho v}{\partial y} dxdydz + \frac{\partial \rho w}{\partial z} dxdydz \tag{3.12}$$

$$0 = \frac{\partial \rho}{\partial t} + \frac{\partial \rho u}{\partial x} + \frac{\partial \rho v}{\partial y} + \frac{\partial \rho w}{\partial z} \tag{3.13}$$

For a steady flow $\left(\partial\rho/\partial t = 0\right)$, the equation (3.13) becomes:

$$0 = \frac{\partial \rho u}{\partial x} + \frac{\partial \rho v}{\partial y} + \frac{\partial \rho w}{\partial z} \tag{3.14}$$

For incompressible flow the equation (3.14) becomes:

$$0 = \frac{\partial u}{\partial x} + \frac{\partial v}{\partial y} + \frac{\partial w}{\partial z} \tag{3.15}$$

For two dimension flow the equation (3.15) becomes:

$$0 = \frac{\partial v}{\partial y} + \frac{\partial w}{\partial z} \tag{3.16}$$

3.4.1.5 Conservation of Momentum:

The principle of conservation of mass indicates that in the absence of any external force acting on a body .the body retains its total momentum.

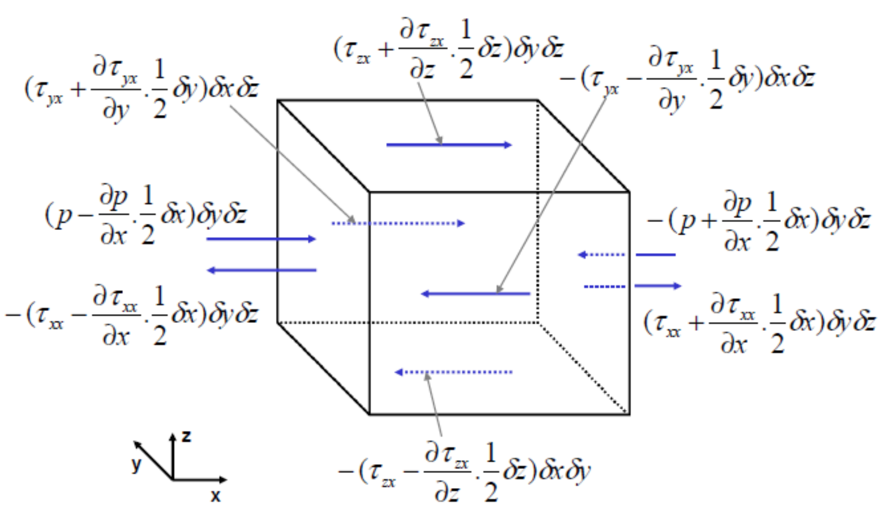

Figure 3.6 Infinitesimally small, moving fluid element. Only the forces in the x direction are shown.

Using newton's second law:

$$\sum F = ma \tag{3.17}$$

Force in the $x-$direction:

$$dF_x = dm_x a_x \tag{3.18}$$

Force in the $y-$direction:

$$dF_y = dm_y a_y \qquad (3.19)$$

Force in the $z-$direction:

$$dF_z = dm_z a_z \qquad (3. 20)$$

There is two type of forces acting on the particle surface force and body force. Substitute this terms in the equation:

$$F_{surface} + F_{body} = ma \qquad (3.21)$$

The body force in the $x-$direction:

$$\left(dF_b\right)_x = dmg_x \qquad (3.22)$$

The body force in the $y-$direction:

$$\left(dF_b\right)_y = dmg_y \qquad (3.23)$$

The body force in the z– direction:

$$\left(dF_b\right)_z = dmg_z \qquad (3.24)$$

While the surface forces:

The surface force in the $x-$direction:

$$\left(dF_s\right)_x = \left(\frac{\delta\sigma_{xx}}{\delta x} + \frac{\delta\tau_{yx}}{\delta y} + \frac{\delta\tau_{zx}}{\delta z}\right)dxdydz \qquad (3.25)$$

The surface force in the y– direction:

$$\left(dF_s\right)_y = \left(\frac{\delta\sigma_{yy}}{\delta y} + \frac{\delta\tau_{xy}}{\delta x} + \frac{\delta\tau_{zy}}{\delta z}\right)dxdydz \qquad (3.26)$$

The surface force in the z – direction:

$$\left(dF_s\right)_z = \left(\frac{\delta\sigma_{zz}}{\delta z} + \frac{\delta\tau_{xz}}{\delta x} + \frac{\delta\tau_{yz}}{\delta y}\right)dxdydz \tag{3.27}$$

While

$$m = \rho dxdydz \tag{3.28}$$

The equation (3.21) in the x – direction after substitute equations (3.18 , 3.22,3.25) becomes:

$$\left(\frac{\delta\sigma_{xx}}{\delta x} + \frac{\delta\tau_{yx}}{\delta y} + \frac{\delta\tau_{zx}}{\delta z}\right)dxdydz + \rho dxdydzg_x = \rho dxdydz\left(\frac{\partial u}{\partial t} + u\frac{\partial u}{\partial x} + v\frac{\partial u}{\partial y} + w\frac{\partial u}{\partial z}\right) \tag{3.29}$$

Reducing the equation (3.28) to:

$$\left(\frac{\delta\sigma_{xx}}{\delta x} + \frac{\delta\tau_{yx}}{\delta y} + \frac{\delta\tau_{zx}}{\delta z}\right) + \rho g_x = \rho\left(\frac{\partial u}{\partial t} + u\frac{\partial u}{\partial x} + v\frac{\partial u}{\partial y} + w\frac{\partial u}{\partial z}\right) \tag{3.30}$$

The equation in the y – direction becomes:

$$\left(\frac{\delta\sigma_{yy}}{\delta y} + \frac{\delta\tau_{xy}}{\delta x} + \frac{\delta\tau_{zy}}{\delta z}\right) + \rho g_y = \rho\left(\frac{\partial v}{\partial t} + u\frac{\partial v}{\partial x} + v\frac{\partial v}{\partial y} + w\frac{\partial v}{\partial z}\right) \tag{3.31}$$

The equation in the z – direction becomes:

$$\left(\frac{\delta\sigma_{zz}}{\delta z} + \frac{\delta\tau_{xz}}{\delta x} + \frac{\delta\tau_{yz}}{\delta y}\right) + \rho g_z = \rho\left(\frac{\partial w}{\partial t} + u\frac{\partial w}{\partial x} + v\frac{\partial w}{\partial y} + w\frac{\partial w}{\partial z}\right) \tag{3.32}$$

And these three equations are the Navire – stocks equations.

3.4.1.6 Conservation of Energy:

First law of thermodynamics: rate of change of energy of a fluid particle is equal to the rate of heat addition plus the rate of work done.

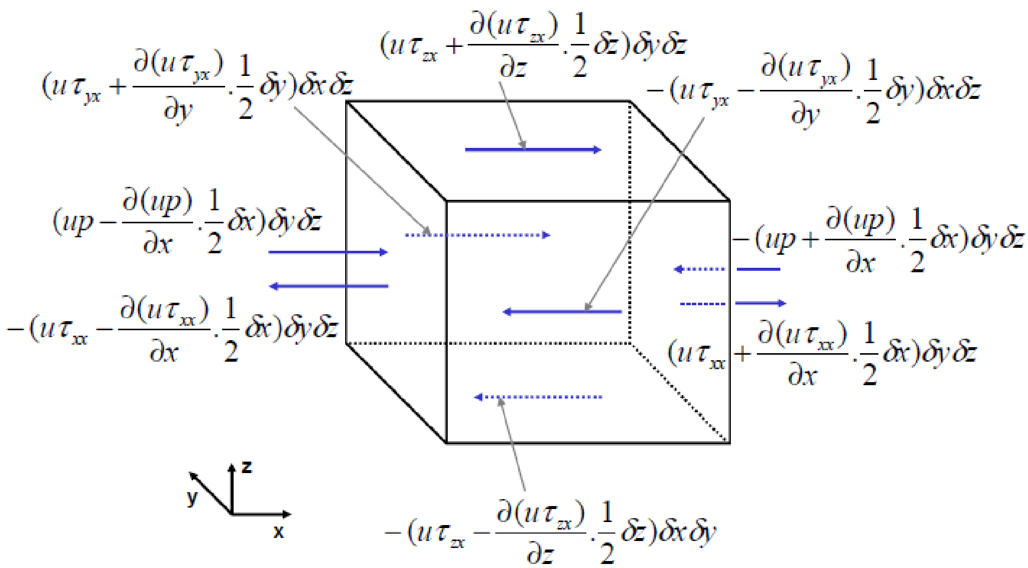

Figure 3.7 Energy fluxes associated with an infinitesimally small, moving fluid element. For simplicity, only the fluxes in the x direction are shown.

Net rate of work done by pressure in the *x*-direction is:

$$\left(up-\left(up+\frac{\partial(up)}{\partial x}dx\right)\right)dydz=-\frac{\partial(up)}{\partial x}dxdydz \tag{3.33}$$

The net rate of work done by the shear stresses in the *x*-direction:

$$\left(u\tau_{xy}-\left(u\tau_{xy}+\frac{\partial(u\tau_{xy})}{\partial x}dx\right)\right)dydz=-\frac{\partial(u\tau_{xy})}{\partial x}dxdydz \tag{3.34}$$

The net rate of work done on the moving fluid element due to these forces:

$$=\left(-\frac{\partial(up)}{\partial x}+\frac{\partial \tau_{xx}}{\partial x}+\frac{\partial \tau_{yx}}{\partial y}+\frac{\partial \tau_{zx}}{\partial z}\right) \quad (3.35)$$

The net rate of work done on the moving fluid element is the sum of the surface force contributions in the *x*-, *y*- and *z*-directions, as well as the body force contribution:

$$\left[\begin{array}{l}-\left(\frac{\partial(up)}{\partial x}+\frac{\partial(vp)}{\partial y}+\frac{\partial(wp)}{\partial z}\right)+\frac{\partial(u\tau_{xx})}{\partial x}+\frac{\partial(u\tau_{yx})}{\partial y}+\frac{\partial(u\tau_{zx})}{\partial z}+\frac{\partial(v\tau_{yy})}{\partial y}\\ +\frac{\partial(v\tau_{xy})}{\partial y}+\frac{\partial(v\tau_{zx})}{\partial z}+\frac{\partial(w\tau_{zz})}{\partial z}+\frac{\partial(w\tau_{yz})}{\partial y}+\frac{\partial(w\tau_{xz})}{\partial x}\end{array}\right]dxdydz+\rho\vec{f}.\vec{V}dxdydz$$

(3.36)

The net flux of heat into the element = Volumetric heating of the element

$$=\rho\dot{q}dxdydz \quad (3.37)$$

The net heat transferred in the *x*-direction into the fluid element by thermal conduction:

$$\left(\dot{q}_x-\left(\dot{q}_x+\frac{\partial\dot{q}_x}{\partial x}dx\right)\right)dydz=\frac{\partial\dot{q}_x}{\partial x}dxdydz \quad (3.38)$$

Taking into account heat transfer in the *y*- and *z*-directions across the other faces:

The Heating of the fluid element by thermal conduction equals:

$$-\left(\frac{\partial\dot{q}_x}{\partial x}+\frac{\partial\dot{q}_y}{\partial y}+\frac{\partial\dot{q}_z}{\partial z}\right)dxdydz \quad (3.39)$$

Net flux of heat into the element equals:

$$\left(\rho\dot{q}_x-\left(\frac{\partial\dot{q}_x}{\partial x}+\frac{\partial\dot{q}_y}{\partial y}+\frac{\partial\dot{q}_z}{\partial z}\right)\right)dxdydz \qquad (3.40)$$

While:

$$\dot{q}_x=-k\frac{\partial T}{\partial x} \qquad (3.41)$$

$$\dot{q}_y=-k\frac{\partial T}{\partial y} \qquad (3.42)$$

$$\dot{q}_z=-k\frac{\partial T}{\partial z} \qquad (3.43)$$

Net flux of heat into the element:

$$\left(\rho\dot{q}_x-\left(\frac{\partial}{\partial x}\left(k\frac{\partial T}{\partial x}\right)+\frac{\partial}{\partial y}\left(k\frac{\partial T}{\partial y}\right)+\frac{\partial}{\partial z}\left(k\frac{\partial T}{\partial z}\right)\right)\right)dxdydz \qquad (3.44)$$

Rate of change of energy inside the fluid element:

$$\rho\frac{D}{Dt}\left(e+\frac{V^2}{2}\right)dxdydz \qquad (3.45)$$

The final form of the energy equation is:

$$\rho\frac{D}{Dt}\left(e+\frac{V^2}{2}\right)=\rho\dot{q}_x+\frac{\partial}{\partial x}\left(k\frac{\partial T}{\partial x}\right)+\frac{\partial}{\partial y}\left(k\frac{\partial T}{\partial y}\right)+\frac{\partial}{\partial z}\left(k\frac{\partial T}{\partial z}\right)+\frac{\partial(u\tau_{xx})}{\partial x}+\frac{\partial(u\tau_{yx})}{\partial y}+$$
$$\frac{\partial(u\tau_{zx})}{\partial z}+\frac{\partial(v\tau_{yy})}{\partial y}+\frac{\partial(v\tau_{xy})}{\partial y}+\frac{\partial(v\tau_{zx})}{\partial z}+\frac{\partial(w\tau_{zz})}{\partial z}+\frac{\partial(w\tau_{yz})}{\partial y}+\frac{\partial(w\tau_{xz})}{\partial x}+\rho\vec{f}.\vec{V}$$

(3.46)

3.5 The Discretization Process:

The numerical solution of partial differential equation consist of finding the values of dependent variable ϕ at specified point from witch its distribution over the domain of interest can be constructed . These points are called grid elements or grid nodes and result from the discretization of original geometry into a set of non-overlapping discrete elements. In all methods the focus is on replacing the continuous exact solution of the partial equation with discrete values.

3.5.1 Steps of Discretization Processes:

Step 1: Geometric and physical modeling:

A mathematical formulation of a physical phenomenon to consider and understand this phenomenon .there tow levels of modeling are performed the first one in relation to the geometry of the physical domain and the second one in relation to the physical phenomena of interest. Physical components may be removed or replaced with appropriate mathematical representations.

Step 2: Domain discretization:

Subdivision of the physical domain into discrete non-overlapping cells or elements that completely fill the computational domain to yield a grid or mesh system. The mesh is composed of discrete element defined by a set of vertices and bounded by faces [4].

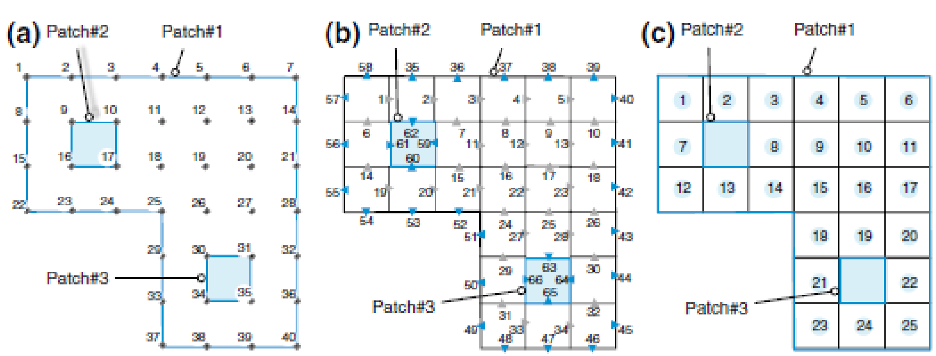

Figure 3.8 (a) Mesh vertices, (b) faces, and (c) elements.

During discretization, the partial differential equations are integrated over each element in the mesh resulting in a set of algebraic equations with each one linking the value of the variable at an element to the values at its neighbors. The algebraic equations are then assembled into global matrices and vectors and the coefficients of every equation stored at the row and column locations corresponding to the various element indices. The integration of the equations over each element is referred to as local assembly while the construction of the overall system of equations from these contributions is referred to as global assembly.

Step 3: Equation discretization

In this step partial differential equations, are transformed into a set of algebraic equations, one for each element in the computational domain. These algebraic equations are then assembled into a global matrix and vectors.

Step 4: solution of the discretized equation

The discretization of the differential equation results in a set of discrete algebraic equations, which must be solved to obtain the discrete values. The techniques to solve this algebraic system of equations are independent of the discretization method, and represent the various trajectories that can be followed to obtain a solution.

3.6 Techniques for Numerical Discretization:

Discretization process is used to solve the governing equation of the fluid motion by generate their numerical analogue. In this process each term within the partial differential equation describing the flow is written in such a manner that the computer can be programmed to calculate. The most three commonly used techniques are: The finite difference method, the finite element method, and the finite volume method.

3.6.1 The Finite Difference Method:

Utilization of the Taylor series to discretize the derivative of dependent variable, e.g., velocity *u*, with respect to the independent variable, e.g., special coordinated *x*, consider the curve the curve in Fig.(3.9) which represent the variation of *u* with *x i.e., u(x)*. After discretization, the curve u(x) can be represented by a set of discrete points, u_i 's. These points can be related to each other using Taylor series expansion. Consider two points, ($i+1$) and ($i-1$), a small distance Δx from the central point, (i).

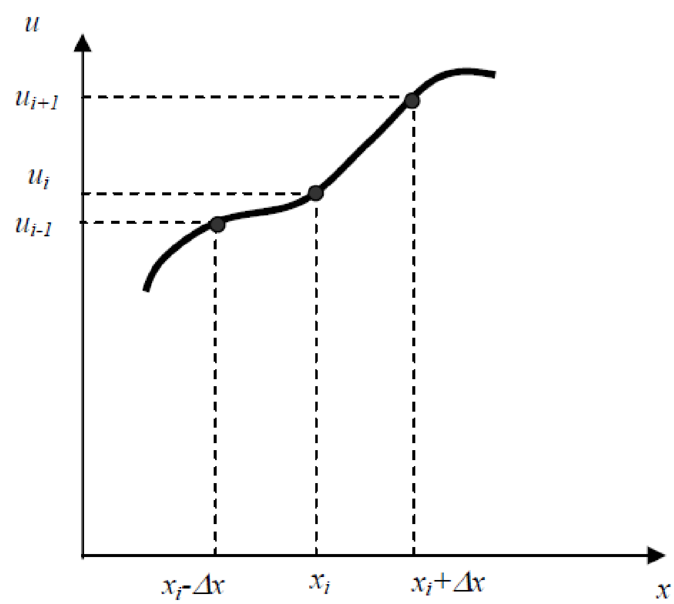

Figure 3.9 Location of points for Taylor series.

Difference formulae are classified in two ways: (1) by the geometrical relationship of the points, namely, central, forward, and backward differencing; or (2) by the accuracy of the expressions, for instance, central difference is second-order accurate. We can obtain higher order approximations by applying the Taylor series expansion for more points.

3.6.2 The Finite Element Method:

The fluid domain under consideration is divided the fluid domain under consideration into finite number of sub-domains "elements". The summation of variation of the variable in each element is used to describe the whole flow field.

Consider the two nodded element shown in Figure (3.10), in which variable *u* varies linearly inside the element. The end points of the element are called the nodes of the element. For a linear variation of *u*, the first derivative of *u* with respect to *x* is simply a constant. If *u* is assumed to vary linearly inside an element, we cannot define a second derivative for it.

Since most fluid problems include second derivative, the following technique is designed to overcome this problem. First, the partial differential equation is multiplied by an unknown function, and then the whole equation can be integrated over the domain in which it applies. Finally the terms that need to have the order of their derivatives reduced are integrated by parts. This is known as producing a variational formulation.

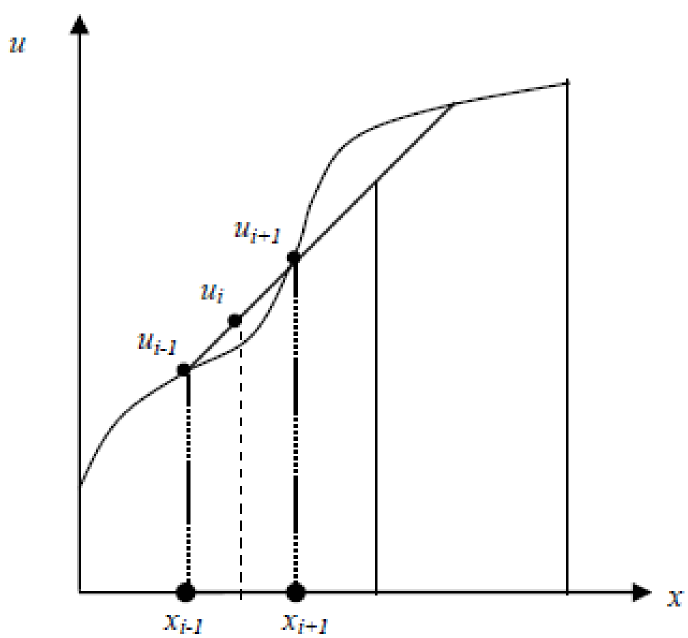

Figure 3.10 A two nodded linear element.

3.6.3 The Finite Volume Method:

It is special case of finite element when the function W is equal to 1 everywhere in the domain, and can resolve some of the difficulties that the other two methods have so it is the most popular method in CFD. This technique is discussed in detail by Patankar.

A typical finite volume, or cell, is shown in Fig.(3.11).point P is the centroid of the volume and the reference point at which we want to discretize the partial differential equation.

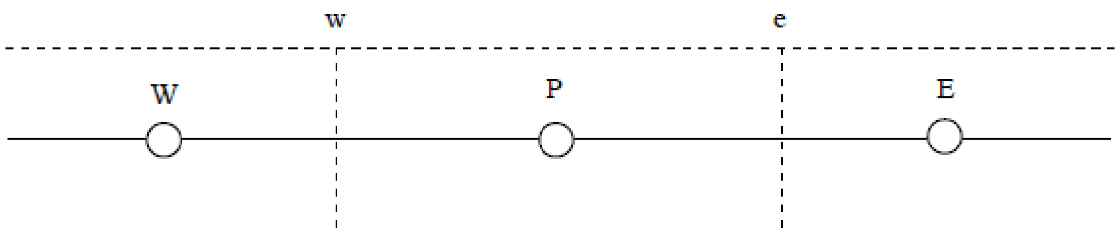

Figure 3.11 A finite volume in one dimension.

W is the volume to the west side, and E the volume to the east side of the volume P. For the one-dimensional finite volume, the volume with centroid P, has two boundary faces at w and e.

3.7 Turbulence Model:

Several turbulence models based on the Boussinesq hypothesis have been developed to express the turbulent viscosity, μ_t, in terms of a velocity $\left(\sqrt{k}\right)$ and length (l) scales such that:

$$\mu_t = \rho l \sqrt{k} \tag{3.47}$$

These models are grouped, into four main categories:

• Algebraic (Zero-Equation) Models.

• One-Equation Models.

• Two-Equation Models.

• Second-Order Closure Models.

In this project I adopt the two equation model.

Two-Equation Turbulence Models, (standard $k-\varepsilon$ model):

The $k-\varepsilon$ model, is based on the Boussinesq approximation with the turbulent viscosity μ_t and thermal diffusivity k_t formulated as:

$$\mu_t = \rho C_\mu \frac{k^2}{\varepsilon} \tag{3.48}$$

$$k_t = \frac{c_p \mu_t}{\Pr_t} \tag{3.49}$$

Where ε is the rate of dissipation of turbulence kinetic energy per unit mass due toviscous stresses given by:

$$\varepsilon = \frac{\mu}{2\rho} \overline{\left\{\nabla v' + \left(\nabla v'\right)^T\right\} : \left\{\nabla v' + \left(\nabla v'\right)^T\right\}} \tag{3.50}$$

In the model, the turbulent kinetic energy k and the turbulent energy dissipation rate ε are computed using

$$\frac{\partial}{\partial t}(\rho k) + \nabla.(\rho \,\mathrm{vk}) = \nabla.(\mu_{eff\,,\mathrm{k}} \nabla k) + \underbrace{P_k - \rho\varepsilon}_{S^k} \tag{3.51}$$

$$\frac{\partial}{\partial t}(\rho\varepsilon) + \nabla.(\rho \,\mathrm{v}\, \varepsilon) = \nabla.(\mu_{eff\,,\varepsilon} \nabla \varepsilon) + \underbrace{C_{\varepsilon 1} \frac{\varepsilon}{k} P_k - C_{\varepsilon 2} \rho \frac{\varepsilon^2}{k}}_{S^\varepsilon} \tag{3.52}$$

Where:

$$\mu_{eff,\mathrm{k}} = \mu + \frac{\mu_t}{\sigma_k} \mu_{eff,\varepsilon} = \mu + \frac{\mu_t}{\sigma_\varepsilon} \qquad (3.53)$$

The compact form of the production of turbulent energy term is given by

$$P_k = \tau^R : \nabla v \qquad (3.54)$$

The flow is assumed to be fully turbulent and the effects of molecular viscosity to be negligible. Therefore the standard k − ε model is a high Reynolds number turbulence model valid only for fully turbulent free shear flows that cannot be integrated all the way to the wall.

Chapter Four

ANSYS Simulation and Result Analysis

4.1 Introduction:

In these chapter the simulation results on ANSYS cfx software will be discussed. Two cases was processed and gets the simulation results of it. The two cases are. The first one a simple car model without additions. The second one care model with underbody tunnel.

The CFD simulation method is preferred on the experimental method (wind tunnel). Due to some rezones. Firstly the accuracy of CFD method is higher. Secondly the time consumed in process is much lower, moreover the wind tunnel takes three to four weeks to arrange a session in it. While in CFD method more 100 simulation can performed in the same time. Finally in some cases there is a critical areas are designed nearly entirely. Which is very difficult to evaluate in wind tunnel. But can be evaluate in CFD easily.

4.2 Car Model:

A simple sadden car model was drawn on Solidworks software, which is shown in figure (4.1).

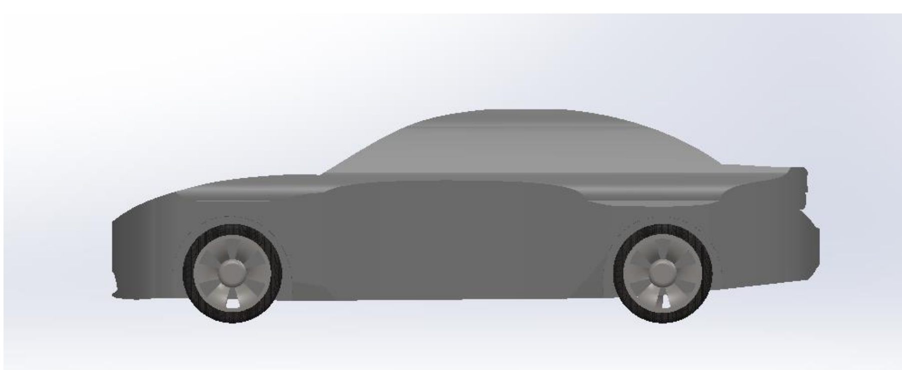

Figure 4.1: car model.

4.3 Tunnel Design:

The Design of tunnel depends on Bernoulli principle. Which states that an increase in the speed of a fluid occurs simultaneously with a decrease in pressure or a decrease in the fluid's potential energy. The principle was applied in the project in this way. Controlling the speed under the car by designing the tunnel in form similar to venture tunnel as shown in figure (4.7). In order to decrease pressure which leads to increase the down force.

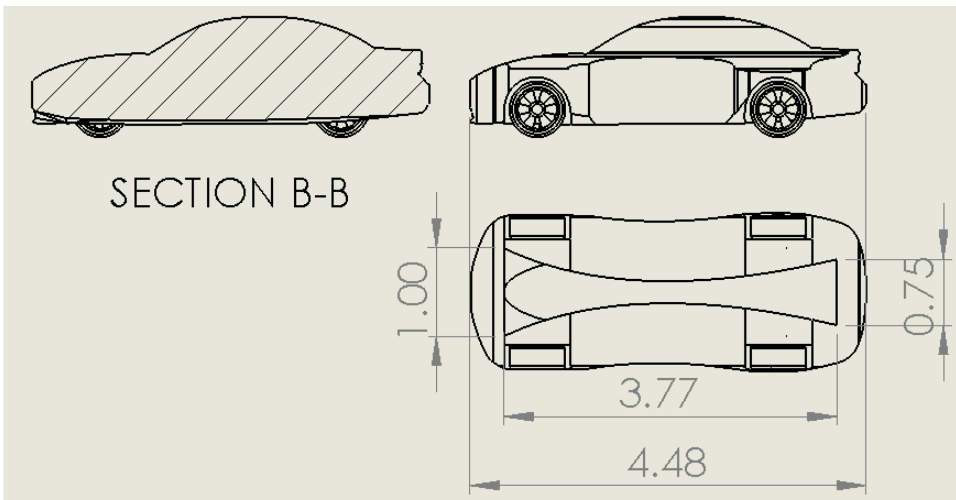

Figure 4.2: Tunnel design.

4.4 Process Procedure:

To get the final results in ANSYS. A procedures should be followed. The first procedure is preprocess, in this stage the model is prepared to the second stage which is the process the solution is performed to get the results. Figure (4.2) shows the sequence of processes in ANSYS workbench, which will be discussed in this section.

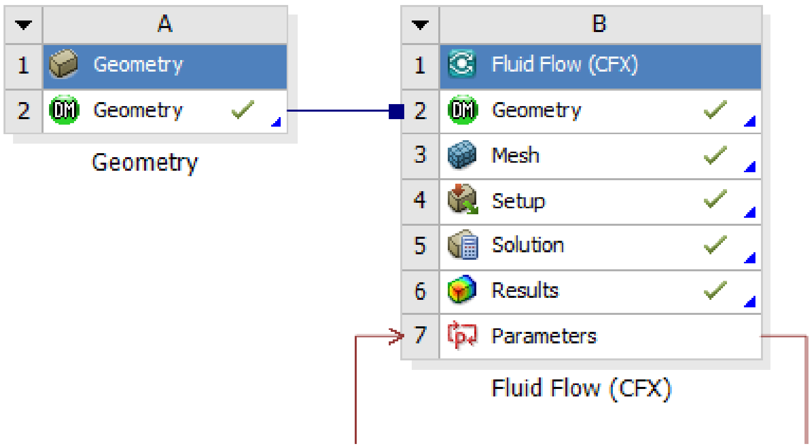

Figure 4.3: Sequence of processes in ANSYS.

First step importing the car model in ANSYS. Importing the geometry to ANSYS can obtained by more than one way. One of these ways is transforms the formula from solid works formula or any other sketching software to igs formula. Or ideating ANSYS settings and made a direct connection between ANSYS and Solidworks.

After importing the car model in ANSY geometry. Computational domain (enclosure) should be created around the car which represent the wind tunnel in actual. The dimensions of the computational domain shown in table (4.1).

Table (4.1) Computational domain.

X	Y	Z
1.5m	2m	3m
-1.5m	0.2m	-3m

The next step, meshing the model. The meshing should be correct and suitable to give accurate result where's wrong meshing gives incorrect solution. And should be fine as much as possible. Especially around the model which is the area of attention, in which the interaction of air molecules with the car. And this shown in figure (4.3).

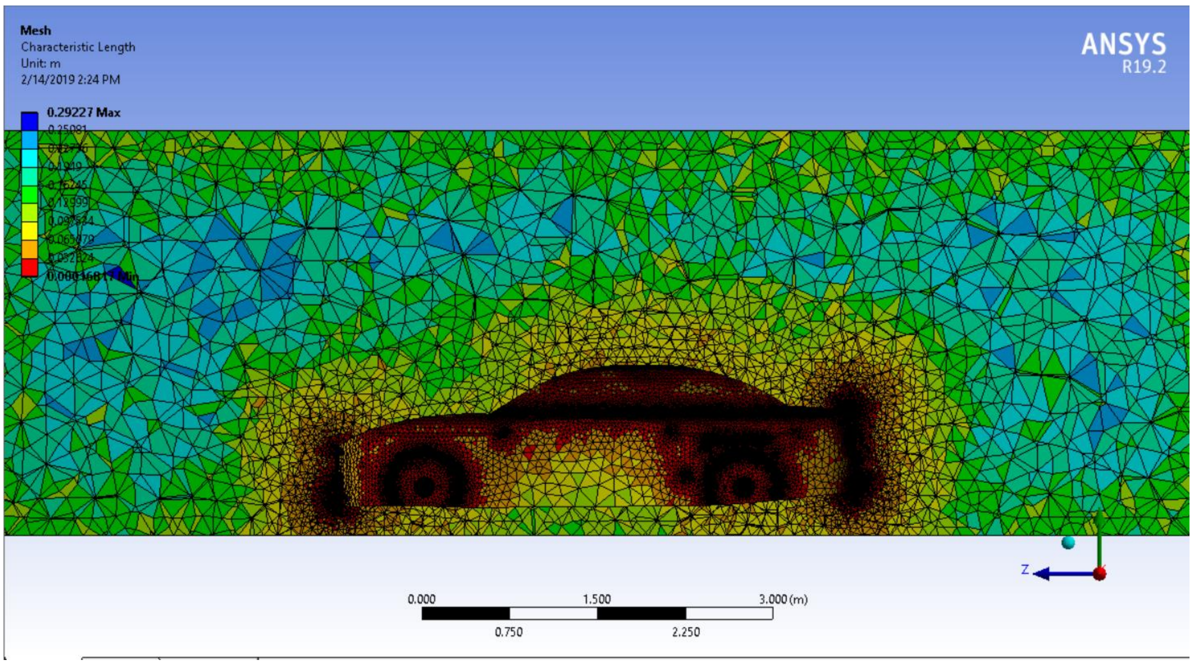

Figure 4.4: Car model after meshing process.

Third step setting up. In these step the boundary conditions will be determined as shown in table (4.2).

According to the data from table (4.2) and figure (4.4), the car is travelling at a constant speed w forward and the air assumed to be still. These case equivalent to placing a stationary car in the air with a free stream speed w moving against the car towards the positive z direction. The ground also moves together with air in the same speed.

Table 4.2: Boundary conditions.

name	Boundary type	location	Boundary details
Inlet	inlet	Inlet	Normal speed, fore cases:60Km/s,90Km/s, 120Km/s and200Km/s. Flow regime: subsonic, turbulence: medium (intensity = 5%).
Car	wall	Car	Mass and momentum: no slip wall. Wall roughness: smooth wall.
Open	opening	Sky, side plane, back plane.	Flow regime: subsonic, turbulence: medium (intensity = 5%). Mass and momentum: opening pre, 1(atm).
Wall	wall	Ground	Wall U=0,wall V=0,wall W=60Km/s.

.

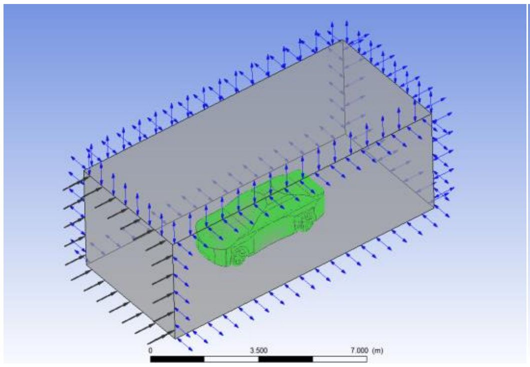
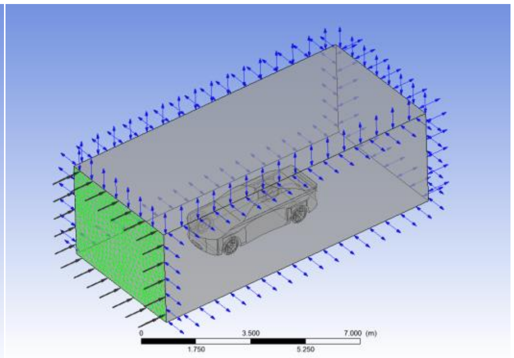

Car Inlet

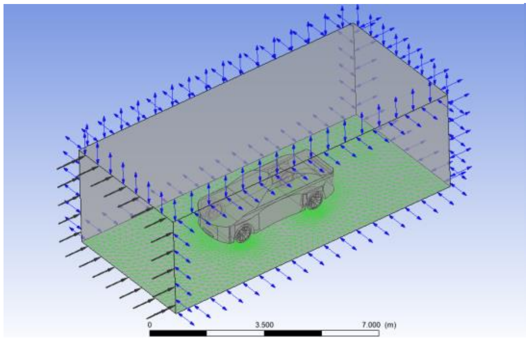
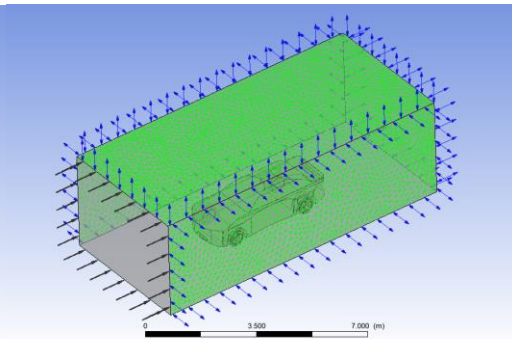

Ground Open

Figure 4.5: Boundary conditions.

4.5 Result Analysis and Discussion:

After finishing the three preprocess steps. The model was ready to do the forth step, which is the solution to get the results.

The focus in results were on aerodynamic characteristic drag force and down force, also in pressure and velocity contours.

The discussion of results on this section as the following, pressure and velocity contours with and without tunnel, finally drag and down force.

4.5.1 Pressure Contour and Velocity Contour for Car Model without Tunnel:

According to figure (4.5), a high pressure can be noticed at the front of the car and at the edges. This increase in pressure at these areas. Because the air slows down when it approaches the front of the car and results in that more air molecules are accumulated into a smaller space. Once the air stagnates in front of the car, it seeks a lower pressure area, such as the sides, top and the bottom of the car. As the air flows over the car hood, pressure is decreasing, but when reaches the front windshield, it increases briefly. When the higher-pressure air in front of the windshield travels over the windshield and top of the car, it accelerates, due to the surface soothe which acquires kinetic energy to air molecules. Causing the decrease of the pressure. This lower pressure literally produces a lift - force on the car roof as the air passes over it.

Figure (4.6) shows velocity counter around the car. As shown in the figure velocity counter coincides with pressure counter. According to the relation between pressure and velocity, which is inverse relationship. Which appears in the two figures. In pressure counter, high pressure areas meet zero velocity areas in velocity counter.

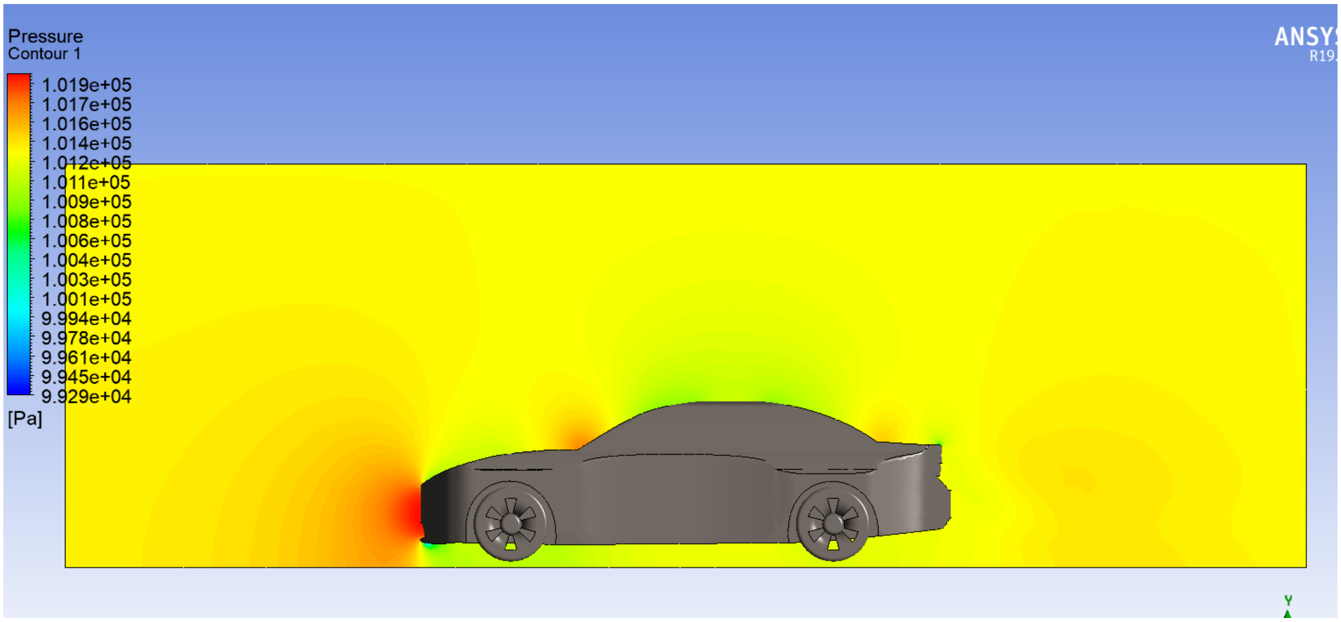

Figure 4.6: Pressure counter before adding under body tunnel

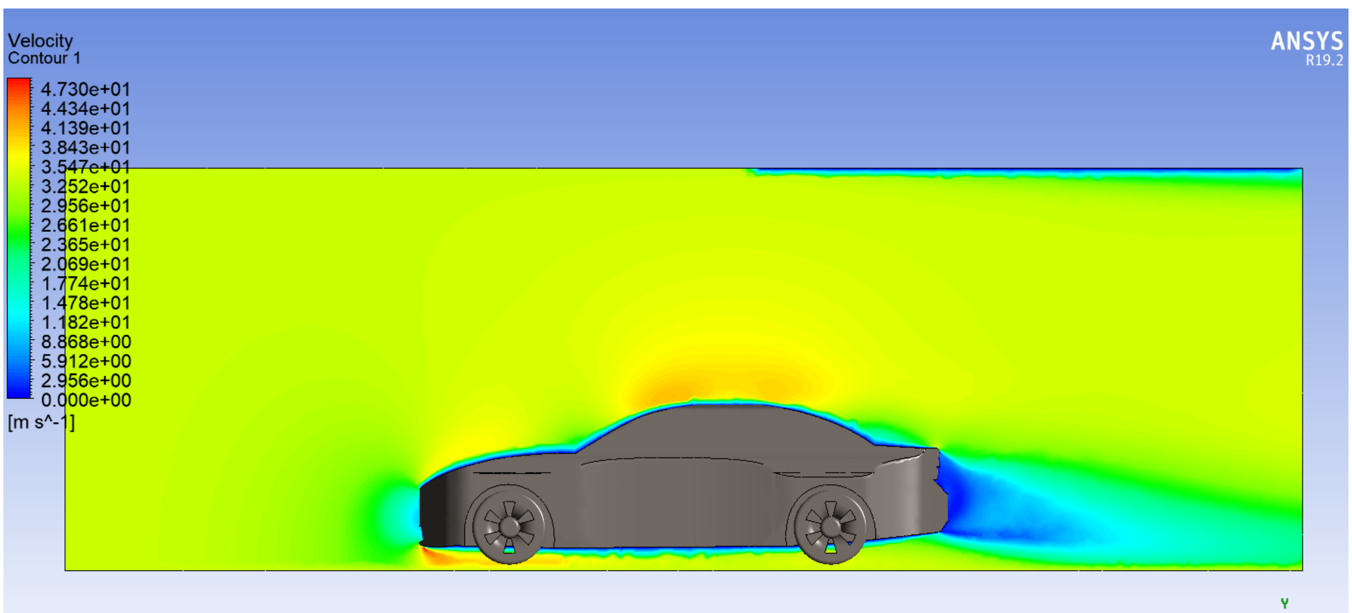

Figure 4.7: Velocity counter before adding under body tunnel

4.5.2 Pressure Contour and Velocity Contour for Car Model with Tunnel:

According to figure (4.8), pressure counter after adding the tunnel similar to the pressure counter before, expect two areas, under and behind the car. The pressure decreased in these areas. The next figure (4.9), which shoes velocity counter. Shows a change in velocity below and behind the car. The velocity increases in these areas and this coincides with the changes in pressure.

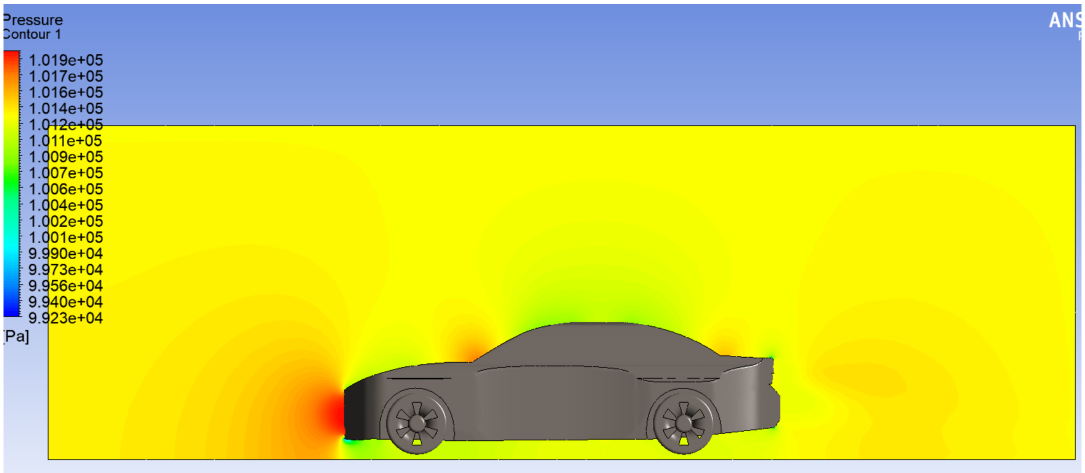

Figure 4.8 Pressure counter after adding under body tunnel.

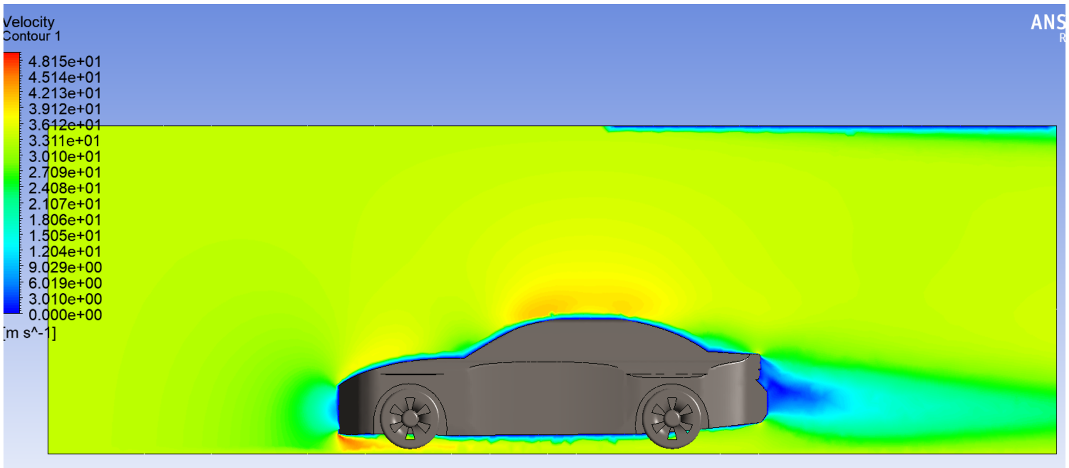

Figure 4.9: Velocity counter after adding under body tunnel.

4.5.3 Drag and Lift Coefficients:

Finally evaluating drag and lift coefficients. To estimate the benefit of the project. Table (4.3) represents drag force and down force for the two cases, before and after adding the tunnel. As shown in the table, the tunnel effect on the down force. The down force increased specially at high speeds (120 Km/h and more). In the other hand the effect on drag force very small. Table (4.4) shoes lift and drag coefficients.

Table 4.3: Drag force and down force.

Velocity	Case 1		Case 2	
	Drag force	Down force	Drag force	Down force
60 Km/h	105.376	51.0226	111.231	65.4874
90 Km/h	244.339	116.227	250.698	125.761
120 Km/h	440.597	148.687	453.744	212.882
200 Km/h	1204.67	391.678	1205.98	593.585

Table 4.4: Drag coefficient and Lift coefficient.

Velocity	Case 1		Case 2	
	Drag coefficient	Lift coefficient	Drag coefficient	Lift coefficient
60 Km/h	0.34	-0.30	0.36	-0.37
90 Km/h	0.35	-0.30	0.36	-0.32
120 Km/h	0.36	-0.21	0.37	-0.30
200 Km/h	0.35	-0.20	0.35	-0.30

4.5.4 Drag Force Curves:

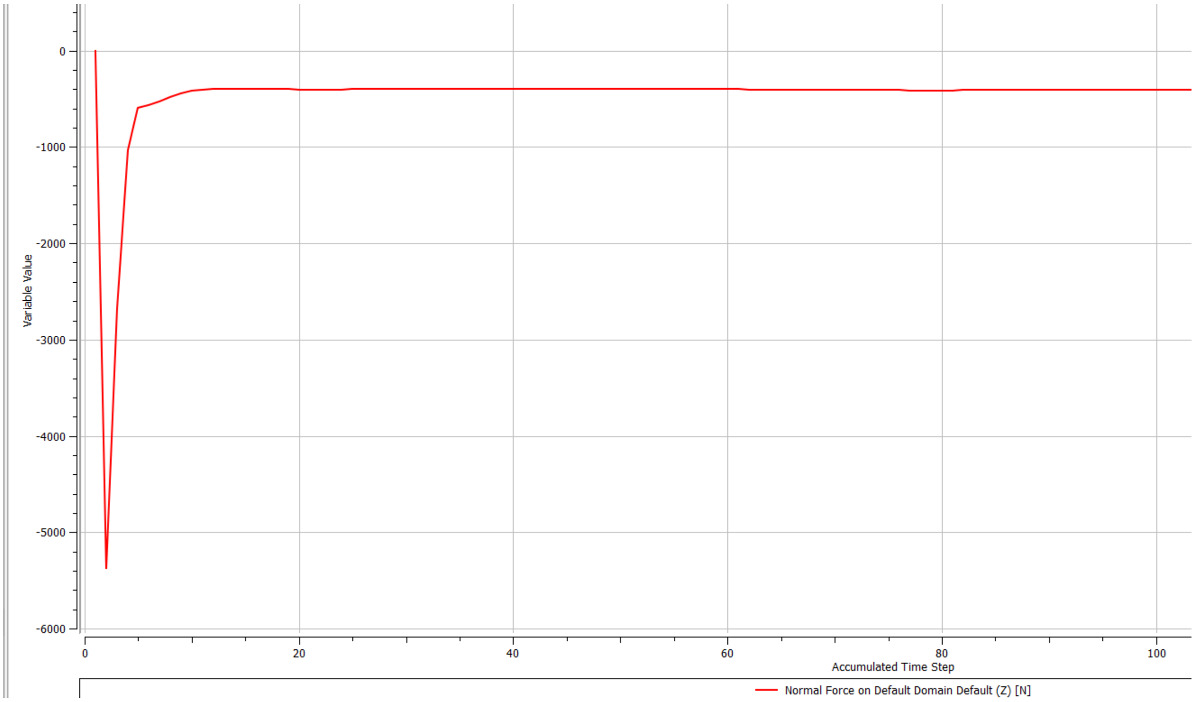

Figure 4.10 Drag force at velocity=120 Km/h (before adding under body tunnel).

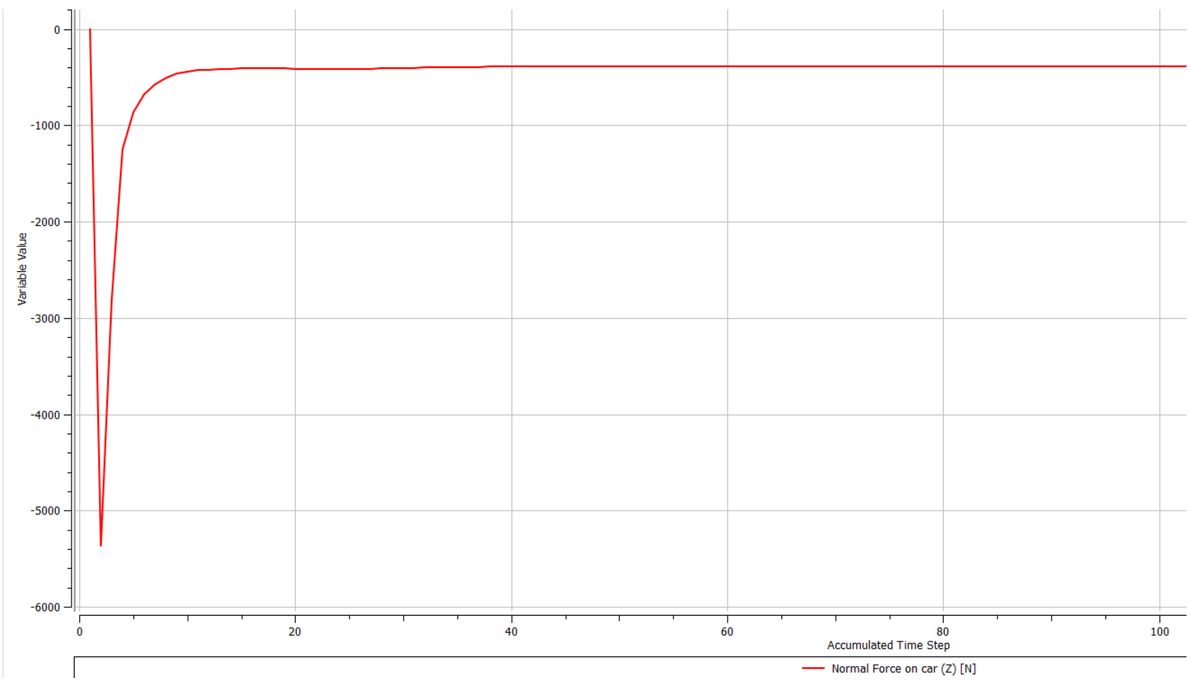

Figure 4.11: Drag force at velocity=120 Km/h (after adding under body tunnel).

4.5.5 down force curves:

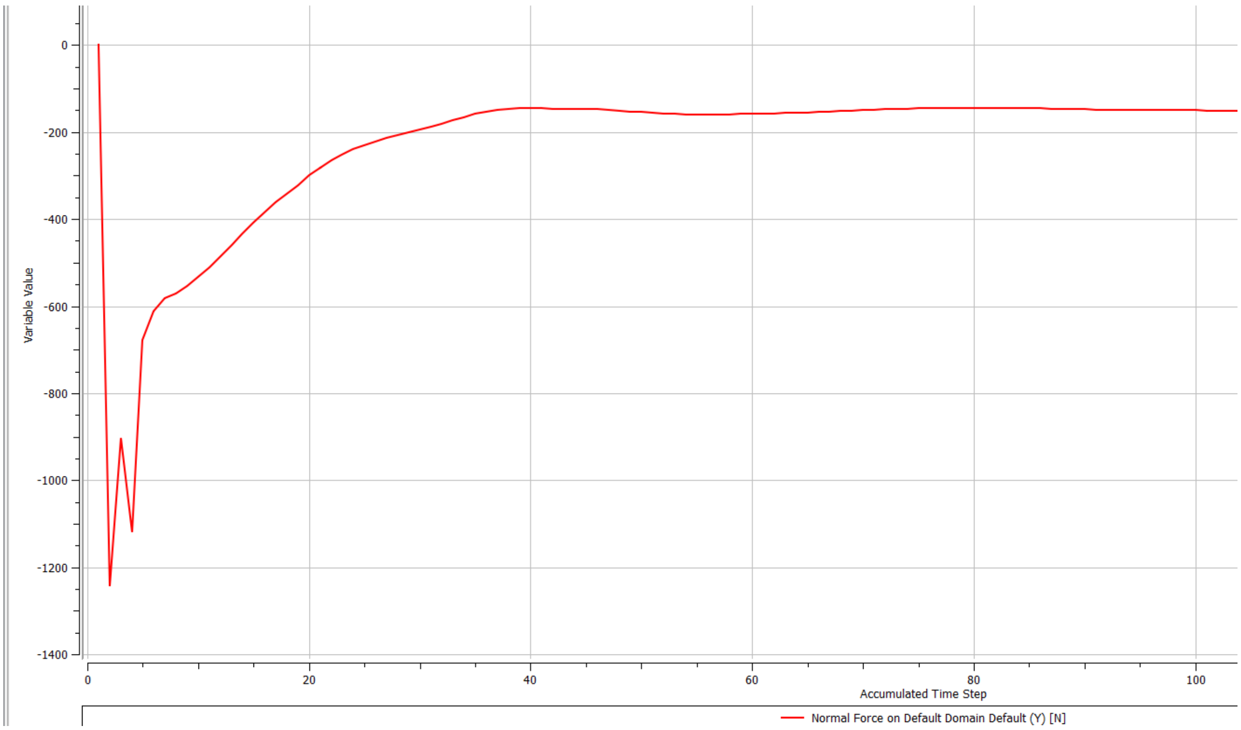

Figure 4.12: Down force at velocity=120 Km/h (before adding under body tunnel).

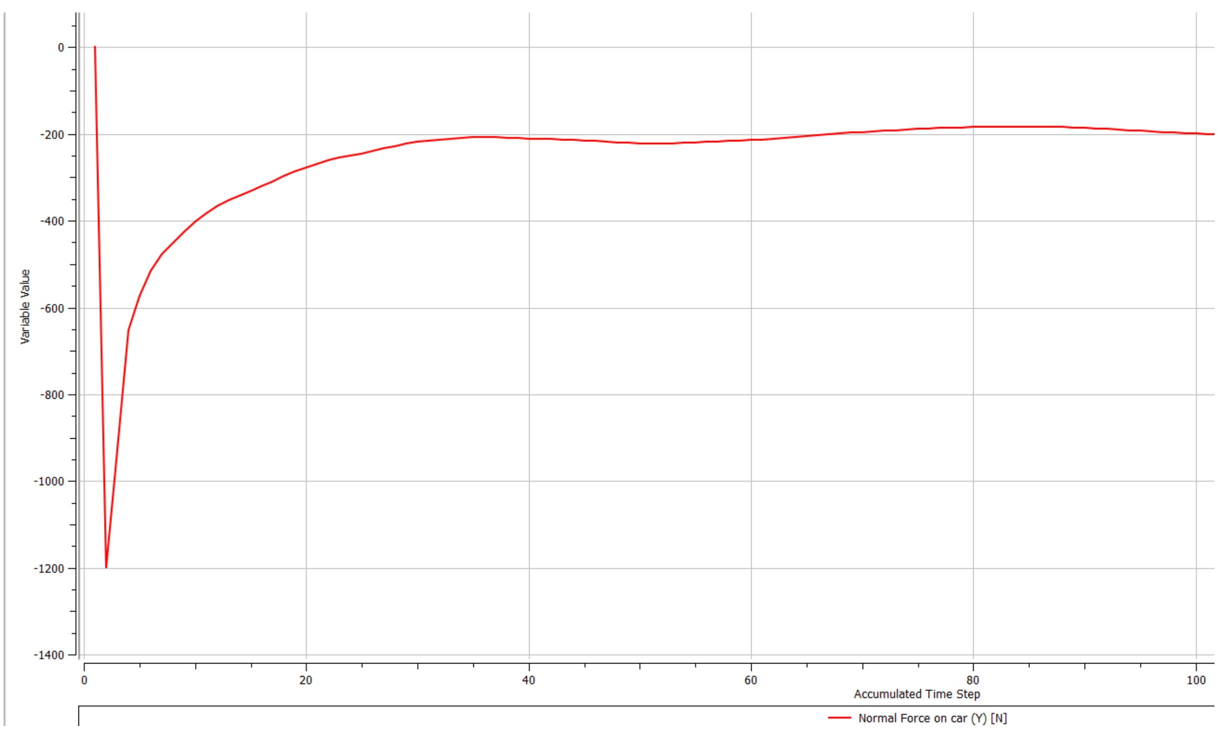

Figure 4.13: Dawn force at velocity=120 Km/h (after adding under body tunnel).

4.6 conclusion:

The results from ANSYS software were proved the effectiveness of the tunnel on vehicle stability. As shown previously the down force was increased, because of the pressure reduction under the vehicle. The pressure reduced as a result of increasing the velocity of flowing air across the tunnel. And this is the required from the project increasing the stability of vehicle by increasing the down force. The side effect of the tunnel was increasing the drag coefficient by (0.01). This small increasing in drag coefficient will cause a small increasing in fuel consumption. Comparing the small increasing in fuel consumption which acquired from the 0.01 gained in drag coefficient, with the 0.07 increasing in lift coefficient. This is a good result, and can be developed in the future.

References:

[1] John Wiley & Sons , Joseph Katz, Automotive aerodynamics San Diego State University,USA,2016

[2] Meinhard T. Schobeiri ,Fluid Mechanics for Engineers, A Graduate Textbook-Springer-Verlag Berlin Heidelberg.2010

[3] Johan Leven, Aerodynamic analysis of drag reduction devices on the underbody for SAAB 9-3 by CFD, Master's Thesis in Automotive Engineering, Sweden.2011

[4] Moukalled, The Finite Volume Method in Computational Fluid Dynamics, Pilar Garcia-Navarro,USA. 2016

[5] G. Siva and V. Loganathan, Design and Aerodynamic Analysis of a Car to Improve Performance, IDOSI Publications. 2016

[6] Járműipari innováció, CFD analysis of concept car in order to improve aerodynamics, University of Osijek, Croatia.2010